TÉCNICO LISBOA

KSHV LANA WIN-like motif influence on *in vivo* persistent infection

Filipa Prata Silva

Thesis to obtain the Master of Science Degree in

Microbiology

Supervisor:

Professor Doutor João Pedro Monteiro e Louro Machado de Simas

Co-supervisor:

Professora Doutora Leonilde de Fátima Morais Moreira

Examination Committee

Chairperson: Professor Doutor Jorge Humberto Gomes Leitão

Supervisor: Professor Doutor João Pedro Monteiro e Louro Machado de Simas

Members of the Committee: Doutora Maria João Lopes Gonçalves de Brito Amorim

October 2021

PREFACE

The work presented in this thesis was performed at Pedro Simas Lab, Instituto de Medicina Molecular João Lobo Antunes, University of Lisbon (Lisbon, Portugal), during the period of September 2020 - September 2021, under the supervision of Professor Doutor Pedro Simas. The thesis was co-supervised at Instituto Superior Técnico by Professora Doutora Leonilde Moreira.

DECLARATION

I declare that this document is an original work of my own authorship and that it fulfills all the requirements of the Code of Conduct and Good Practices of the Universidade de Lisboa.

ACKNOWLEDGEMENTS

I would like to thank my supervisor Dr. Pedro Simas for accepting me in his lab, for believing in me and my skills and for all the advice throughout the development of my work. I would also like to thank my internal supervisor, Dr. Leonilde Moreira, for the availability to answer any questions and for allowing me my independence this year.

A special thanks to all members of PSimas Lab for the support, advice and friendship you've shared with me. In particular, a huge thanks to Andreia and Catarina for always answering my questions and helping me with everything, for the laughs and late nights, for the friendship and for simply being there. You made this year a great experience.

To my brother, mom and dad, thank you for always being ready to listen to me talk about my work even when you didn't understand a thing I was saying.

And last but not least, thank you to all my friends (you know who you are) for the support, commiseration, distractions and laughter.

All of you made it possible for me to finish this thesis. Thank you!

ABSTRACT

Kaposi's sarcoma-associated herpesvirus (KSHV) is an oncogenic herpesvirus, responsible for disease in mostly immunocompromised patients mainly co-infected with HIV. This virus presents a lifelong persistent infection controlled by the latency associated nuclear antigen (LANA) and sporadic lytic reactivation.

During infection, the viral genome forms an episome – a circular and chromatinized DNA molecule – which persists in the cell nucleus tethered to host chromosomes by LANA. This multifunctional protein has also been associated with several chromatin modifications through the interaction with histone modification complexes. Histone methylation marks, both activating (H3K4me3) in latency regions, and repressing (H3K27me3) in lytic regions, have been identified in KSHV chromatin. Interestingly, H3K4me3 marks have also been found in terminal repeats (TRs) DNA, despite there being no ORFs in this genome region. The deposition of this histone modification has been connected with LANA activity, through its interaction with the MLL1 COMPASS complex. This complex includes WDR5 which typically binds to the WIN motif of MLL1. LANA has a WIN-like motif able to bind to WDR5, competing with MLL1 and regulating H3K4me3 deposition. This mark is thought to be a DNA degradation signal (anti-viral host defence mechanism) and its presence in the TRs revolves around the fact that this region is easier to repair from DNAse damage than a critical gene region.

In this study, the relevance of LANA's WIN-like motif was evaluated in an *in vivo* animal model. This involves the use of chimeric MHV-68 (Murine Herpesvirus 68) viruses where the coding region for its mLANA protein has been substituted for the KSHV LANA (kLANA) coding region. The ability of two recombinant viruses with mutations in kLANA WIN motif (one to increase kLANA affinity to WDR5 and one to impair kLANA-WDR5 interaction) to establish a latent infection was evaluated.

It was demonstrated that, *in vivo*, impairing the interaction between kLANA and WDR5 resulted in reduced latency in the spleen, corroborating the mechanism previously described involving WDR5 and MLL1, tri-methylation and viral DNA degradation. Increasing kLANA affinity to WDR5 showed no effects on the establishment of latency.

Further studies should be performed in order to clarify and confirm these results.

Keywords: Kaposi's sarcoma-associated herpesvirus; LANA; chromatin modifications; histone methylation; latency

RESUMO

O herpesvírus associado ao sarcoma de Kaposi (KSHV) é um herpesvírus oncogénico, sendo responsável por causar cancro maioritariamente em pessoas imunocomprometidas, especialmente co-infetadas com VIH. O vírus apresenta uma fase de latência perpétua, regulada pelo antigénio nuclear associado à latência (LANA), interrompida esporadicamente por uma fase lítica.

Durante a infeção, o genoma viral forma um episssoma – uma molécula de DNA circular e com cromatina – que persiste no núcleo de células infetadas ligada aos cromossomas do hospedeiro através da LANA. Esta proteína multifuncional está também associada a modificações da cromatina viral ao interagir com complexos de modificação de histonas. Marcas como a metilação de histonas, tanto marcas ativadoras (H3K4me3), em regiões de latência, como marcas repressoras (H3K27me3), em regiões líticas, foram identificadas no genoma do KSHV. Marcas H3K4me3 foram também encontradas na região de repetições terminais do genoma viral, apesar de esta região não ter ORFs. A aplicação desta modificação de histonas foi associada à atividade da LANA, através da interação com o complexo MLL1 COMPASS. Neste complexo está incluída a proteína WDR5 que se liga normalmente à MLL1 através de um motivo de interação com WDR5 (WIN). Recentemente descobriu-se que a LANA também tem um motivo semelhante ao WIN, sendo capaz de interagir com o WDR5 de através de competição com a MLL1, regulando a deposição de H3K4me3. Pensa-se que esta marca funciona como um sinal para degradação do DNA (sistema de defesa antiviral do hospedeiro) e que a sua presença na região terminal se deve ao facto de esta ser mais fácil de reparar de danos provocados por DNAses do que uma região com genes críticos à sobrevivência do vírus.

Neste estudo procedeu-se à avaliação da relevância do motivo semelhante ao WIN da LANA através de um modelo animal *in vivo*. Este modelo envolve a produção de um vírus MHV-68 (herpesvírus de murganho 68) quimera em que a região que codifica para a sua LANA foi substituída pela região que codifica para a LANA do KSHV (kLANA). A capacidade de dois vírus recombinantes com mutações no motivo WIN da kLANA (um em que se aumentou a afinidade da kLANA pelo WDR5 e outro em que se enfraqueceu a interação entre a kLANA e o WDR5) estabelecerem infeção latente persistente foi avaliada.

Demonstrou-se, *in vivo*, que enfraquecer a interação entre a kLANA e o WDR5 levou a um fenótipo de latência reduzida no baço, corroborando o mecanismo descrito previamente que envolve a MLL1 e a WDR5, a metilação de histonas e a degradação de DNA viral. Aumentar a afinidade entre kLANA e WDR5 revelou não afetar o estabelecimento de latência no baço.

Estudos adicionais deverão ser realizados de forma a confirmar e clarificar estes resultados.

Palavras-Chave: Herpesvírus associado ao sarcoma de Kaposi; LANA; modificações da cromatina, metilação de histonas, latência

INDEX

LIST OF FIGURES

LIST OF TABLES

LIST OF ABBREVIATIONS

AIDS - Acquired Immunodeficiency Syndrome

APS – Ammonium Persulphate

BAC – Bacterial Artificial Chromosome

BAC- – Bacterial Artificial Chromosome without BAC sequences

BAC+ – Bacterial Artificial Chromosome with BAC sequences

BHK-21 – Baby Hamster Kidney cells

CPE – Cytopathic Effect

Cre – Cre recombinase

CWS – Cell Working Stock

d.p.i. – Days post-infection

DBD – DNA Binding Domain

DEV – Duck Enteritis Virus

DMEM – Dulbecco's Modified Eagle Medium

EBV – Epstein-Barr Virus

EDTA – Ethylenediamine Tetraacetic Acid

eGFP – Enhanced Green Fluorescent Protein

FBS – Foetal Bovine Serum

g - Gram

GC – Germinal Centre

GMEM – Glasgow's Minimum Essential Medium

GPT – Guanosine Phosphoribosyl Transferase

h.p.i. – Hours Post-Infection

HCMV – Human Citomegalovirus

HHV-6 – Human Herpesvirus 6

HHV-7 – Human Herpesvirus 7

HHV-8 – Human Herpesvirus 8

HIV – Human Immunodeficiency Virus

HRP – Horse Radish Peroxidase

HSV-1 – Herpes Simplex Virus Type 1

HSV-2 – Herpes Simplex Virus Type 2

HVS – Herpesvirus Saimiri

ICA – Infectious Centre Assay

KICS – KSHV Inflammatory Cytokine Syndrome

KS – Kaposi's Sarcoma

KSHV – Kaposi's Sarcoma-associated Herpesvirus

LANA – Latency-associated Nuclear Antigen

LBS – LANA Binding Site

M - Molar

MCD – Multicentre Castleman's Disease

MHV-68 – Murine Herpesvirus 68

mL – Millilitre

mM - Millimolar

MOI – Multiplicity of Infection

MuHV4 – Murid Herpesvirus 4

NIH-T3T-Cre – fibroblasts that express Cre recombinase

ORF – Open Reading Frame

PBS – Phosphate Buffer Saline

PBS-Tween – Phosphate Buffer Saline with 0.05 % Tween-20

PCR – Polymerase Chain Reaction

PEL – Primary Effusion Lymphoma

PFU – Plaque Forming Unit

qPCR – Quantitative PCR

RBC – Red Blood Cell Lysis Buffer

RRV – Rhesus Monkey Rhadinovirus

RT – Room Temperature

RTA – Replication and Transcription Activator

SDS-PAGE – Sodium Dodecyl Sulphate-Polyacrylamide Gel Electrophoresis

TEMED – Tetramethylethylenediamine

TG – Tris Glycine Buffer

TGS – Tris Glycine SDS Buffer

TPB – Tryptose Phosphate Broth

TR – Terminal Repeats

v-FLIP – Fas-associated death domain-like interleukin-1β-converting enzyme (FLICE)-inhibitory protein

VZV – Varicella-Zoster Virus

WB – Western Blot

WIN – WDR5 Interaction Motif

WSM – Working Stock Media

WT – Wild-Type

YACs – Yeast Artificial Chromosomes

YFP – Yellow Fluorescent Protein

µL – Microliter

µg – Microgram

CHAPTER ONE:

INTRODUCTION

1.1. Herpesviruses

Herpesviruses are among the largest and more complex viral particles, also known as virions, known in nature, comprising more than 200 different viruses identified to date[1,2]. The large viral particles, between 120 nm and 360 nm[3], are composed of an outer lipid envelope containing glycoprotein spikes on the surface, an icosahedral nucleocapsid with 162 capsomers surrounding a linear double-stranded DNA molecule, and a proteinaceous tegument layer that separates the envelope from the nucleocapsid[1,4].

The life cycle of herpesviruses presents two distinct phases: the latent phase and the lytic phase. The lytic cycle corresponds to the expression of the majority of viral genes and the production of viral particles. Latency is when the viral genome is maintained in the nucleus, usually in the form of a closed circularized molecule – the episome – and there is no virion production as only a few viral genes are expressed. Since herpesviruses cannot survive for very long outside the host, they establish lifelong infection via latency, allowing for evasion of the immune system[1]. Lytic reactivation – the process of switching from latent infection to lytic replication – throughout the lifetime of the infected individual leads to the production of virions and infection of new cells, either in the same or in a different host. Typically, if a number of cells exhibit lytic viral activity, disease symptoms may appear[5].

Herpesviruses have been classified into the order *Herpesvirales* since 2009, when their taxonomy was reorganized. This order can be divided into three families, which comprise viruses specific to different animal classes. *Alloherpesviridae* includes viruses associated with amphibians and fish and the *Malacoherpesviridae* family contains mollusc viruses. Finally, mammal, avian and reptile viruses are included in *Herpesviridae*[6].

The *Herpesviridae* family encompasses the nine herpesviruses whose primary hosts are humans and which are known to cause disease. According to their biological properties, the viruses in this family can be classified into three subfamilies[1]. Herpes simplex virus types 1 and 2 (HSV-1 and HSV-2) as well as Varicella-Zoster virus (VZV) and Duck enteritis virus (DEV) belong to *Alphaherpesvirinae*, while human cytomegalovirus (HCMV), human herpesvirus 6 A and B (HHV-6A and HHV-6B), and human herpesvirus 7 (HHV-7) are a part of *Betaherpesvirinae*. The last subfamily is *Gammaherpesvirinae,* which includes both Epstein-Barr virus (EBV) and Kaposi sarcoma-associated herpesvirus (KSHV, or human herpesvirus 8, HHV-8) as well as herpesvirus saimiri (HVS), rhesus monkey rhadinovirus (RRV), and murid herpesvirus 4 (MuHV-4, or Murid herpesvirus-68, MHV-68)[1,3,7].

1.2. KSHV

Kaposi's sarcoma-associated herpesvirus (KSHV), also known as human herpesvirus-8 (HHV-8) was found to be the etiological agent of Kaposi's sarcoma (KS) in 1994[8], becoming the second and most recent gammaherpesvirus to infect humans[9], following EBV[10]. KS can be divided into four different classes: classical KS, which affects mostly elderly men of Jewish ancestry in the Mediterranean region; AIDS-associated KS, closely related to human immunodeficiency virus (HIV) infection and more prevalent in men; endemic KS, which is evenly distributed between men, women and children in Sub-Saharan Africa; and iatrogenic KS, which usually develops in recipients of transplants, due to immunosuppression therapy[11]. The severity of the disease is related to the form in which it presents, with AIDS-associated KS being the most aggressive form[12].

Although it is spread worldwide, KS is not equally distributed throughout the world, with endemic regions showing a much higher seroprevalence than non-endemic regions[12]. This is reflected on the transmission routes which correlate to whether KS is endemic or not[13]. KSHV's major route of transmission is through saliva, especially in areas where KSHV is endemic, as seen in other herpesviruses[9,13]. Other routes include sexual transmission, which is thought to be prevalent in non-endemic areas, although little information is available and further studies are needed, and blood transfusion, though it is rather inefficient[13].

Since the first link between KSHV and KS was made, the virus has also been linked to primary effusion lymphoma (PEL)[14], the plasmablastic variant of multicentric Castleman's disease (MCD)[15], and an inflammatory syndrome known as KSHV inflammatory cytokine syndrome (KICS)[16]. These diseases are more commonly found in immunocompromised individuals, especially those co-infected with HIV[17].

1.2.1. Virion and genome structure

The basic structure of a KSHV viral particle includes a nucleocapsid surrounded by the tegument, which is divided into two difficult to distinguish layers, enveloped by a lipid bilayer, the envelope[11] (Figure 1.1). There are eight different proteins in the tegument[11] and seven different glycoproteins in the envelope structure, five conserved among herpesvirus and two specific to KSHV[18]. Inside the

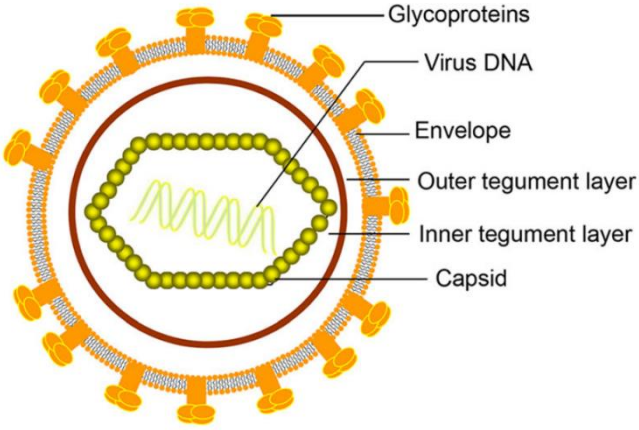

Figure 1.1 – Schematic representation of the KSHV virion. The viral DNA is surrounded by an icosahedral nucleocapsid. The outermost layer is the envelope, a lipid bilayer with embedded glycoproteins, which is separated from the nucleocapsid by an amorphous layer called the tegument[9].

nucleocapsid resides the viral genome, a linear DNA double-strand of approximately 165 kb[17] although it might reach 170 kb[19]. A unique coding region of about 145 kb encodes more than 90 viral proteins, some homologous to human proteins, and many non-coding RNAs, and is flanked by long GC rich terminal repeats (TRs)[12,19]. The KSHV viral genome shares homology with EBV and HVS, other known gammaherpesviruses[7]. As such, the genome annotation was based on the annotation of HVS, with homologous, mostly consecutive, genes from open reading frame (ORF) 4 to ORF75. Additionally, there are KSHV unique genes, which are designated with the prefix K, from K1-K15[11]. The KSHV genome, schematically represented in Figure 1.2, is striking in the number of cellular orthologues which are present (yellow boxes in Figure 1.2)[20].

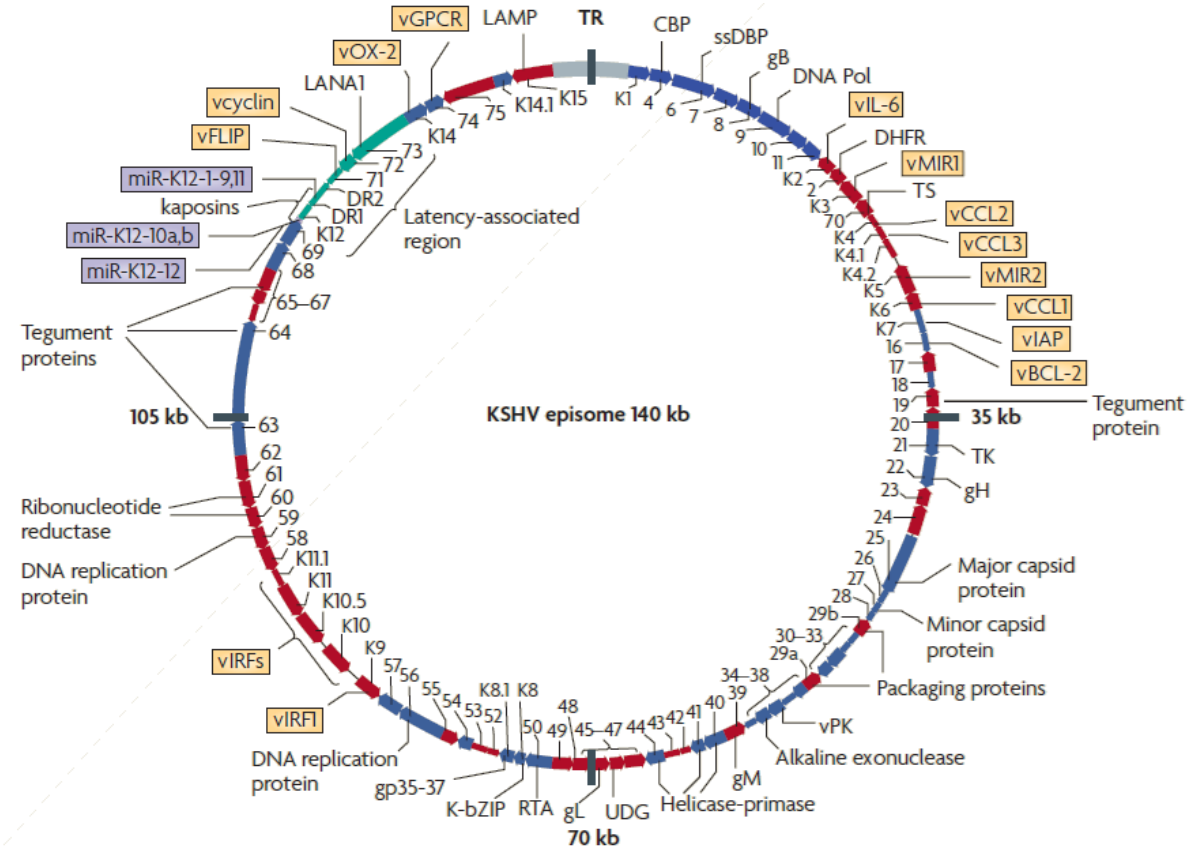

Figure 1.2 – Schematic representation of the KSHV genome. Green indicates the major latency region. Yellow boxes represent cellular orthologues. Adapted from Mesri et al. (2010)[20].

1.2.2. Life cycle

As with other herpesviruses, KSHV presents a biphasic life cycle, with a lytic phase and a latent phase[9,12]. The latent phase is predominant throughout the infection, while the lytic phase is observed as a short-lived reactivation cycle[12]. During latency, very few genes are active and the genome lies in a dormant form in the nucleus. The active genes are grouped together in the latency associated region (Figure 1.2, indicated in green)[21]. The pathologic consequences of KSHV infections are mostly related to latency as most tumour cells harbour latent viral genomes[22]. The lytic phase involves the activation of most viral genes in a predetermined sequence, which leads to the production of viral particles. Therefore, lytic genes can be divided into three kinetic classes, according to the moment when they are expressed: immediate early (IE), early (E) and late (L) genes[21].

The switch between phases is tightly regulated, essentially by two viral proteins: the latency associated nuclear antigen (ORF73, also called LANA) and the replication and transcription activator (ORF50, also called RTA), through fine tuning of their expression levels[12]. RTA is also classified as an IE gene[21] since it is quite important during initial infection[12].

1.2.3. Cell infection

Entry into the cells – the first stage of infection – is a multistep complex process that involves several time-sensitive interactions between cell receptors and viral envelope glycoproteins[7]. KSHV has a broad cell tropism, being able to infect B cells, endothelial cells, epithelial cells and cells of monocyte or macrophage lineage[23]. As such, the cell receptors the virus binds to, as well as the route of entry chosen, vary according to the cell type that is to be infected[7,18].

Following binding to the cell surface, viral particles enter the cell by endocytosis. Two of the four major endocytosis routes have been identified as a route of entry for KSHV in its natural target cells, depending on the type of cell infected. After successful endocytosis of the viral particle, the viral envelope merges with the endocytic vesicle in an acidic environment, freeing the nucleocapsid, which is then trafficked to the nucleus, in as little as 15 minutes, with a peak at the 90-minute mark[7,18].

At this point, the linear DNA undergoes circularization and chromatinization, forming the episome, a stable DNA construct that persists in the nucleus. Circularization, although inefficient, is necessary in order to obtain an intact episome maintenance element consisting of multiple tandem copies of the TRs[24] and is achieved using the infected cell enzymatic machinery[25]. Subsequent chromatinization of the circular DNA serves four distinct purposes while adopting a structure similar to the host genome. Firstly, it ensures the viral DNA is protected against the host DNA damage response. Secondly, during mitosis, it guarantees the stable maintenance, replication, and segregation into daughter cells. Thirdly, it is necessary for the effective completion of the viral lifecycle. And last but not least, it is responsible for the regulation of viral genes, which involves the silencing of the vast majority of genes during latency[25].

Following rapid chromatinization of the viral genome, histone modifications are deposited on the viral chromatin in a biphasic manner allowing for an initial activation of a few lytic genes followed by the establishment of latency through the repression of most viral genes. At first, activating histone modifications like the tri-methylation of the fourth lysine on histone H3 (H3K4me3) or acetylation of the 27th lysine on histone H3 (H3K27ac) are deposited on latency, IE and E promoters peaking at 24 hours post infection (p.i.) and decreasing by 72 hours p.i.[26,27]. Interestingly, TR DNA is also highly enriched in H3K4me3 histone marks[27]. Preliminary results suggest that high levels of this histone mark might be a novel anti-viral host mechanism based on DNA degradation mediated by Dnase1L3, since the loss of viral DNA has been correlated with H3K4me3 levels. It has been suggested that KSHV evolved these histones marks in TRs as a decoy for Dnase activity, since TRs, as repetitive regions, can be more easily repaired through recombination, unlike more unique regions of the genome (unpublished results). Thereafter, repressive histone marks like the tri-methylation on the 27th lysine in histone H3 (H3K27me3) or ubiquitination on the 119th lysine of histone H2A (H2AK119ub) are enriched in the lytic promoters ensuring the transition between a transcriptionally activated state to a repressive state, which results in

the establishment of latency[26,27]. During latency, the RTA (IE) promoter presents a bivalent chromatin with both active (H3K4me3) and repressive (H3K27me3) chromatin modifications, with repressive modifications more prevalent, which would allow for a rapid reactivation of the lytic cycle[27].

Due to the chromatin modifications during the initial stages of infection, there are a few lytic genes that are active at this point, despite the fact that the default pathway of infection is latency[21,26]. This is the case of RTA, for example, the activator of the lytic cycle[21]. Expression of RTA was shown, through a PCR-based analysis, to be highly prevalent within two hours p.i., though it suffered a sharp decline by 24 hours p.i.[28]. In contrast, LANA expression is very low during early infection (2 hours p.i. and up to 6 hours p.i.), but there is a significant increase 24 hours p.i.[12]. The expression of LANA is induced by RTA through binding to the LANA promoter, which explains its transient initial expression [12,21]. LANA is then responsible for the inactivation of most of the lytic genes, promoting the establishment of latent infection[12]. This is unlike what is observed for most herpesviruses, which usually enter a lytic replicative cycle upon cell entry. However, the establishment of latency immediately after infection is similar to the behaviour of EBV[28].

LANA, as its name indicates, is, thus, one of the most important proteins involved in latency of KSHV. In addition, there are a few other proteins and microRNAs that are grouped into the latency associated region that also have a part to play in latency. These include v-cyclin (ORF72), v-FLIP (Fas-associated death domain-like interleukin-1β-converting enzyme (FLICE)-inhibitory protein, K13, ORF71), Kaposin (K12, Kaposins A, B, C), and 25 mature microRNAs (miRNAs)[11].

1.3. KSHV LANA

LANA from KSHV (also called kLANA) is a multifunctional nuclear protein consisting of 1162 amino acid residues[29] with a theoretical molecular mass of 135 kDa, which contrasts with the molecular weight of 220-230 kDa obtained through Western Blot analysis[30]. This protein has two nuclear localization signals, one in the N-terminal and one in the C-terminal and can be divided into several regions[30]. In the N-terminal there is a proline rich region (P). The central region encompasses an aspartic acid and glutamic acid repeat region (DE), a glutamine rich region (Q), a glutamine and glutamate region (EQE), and a putative leucine zipper (LZ), all of which contain repeat elements. This region can vary in size between KSHV isolates. The C-terminal comprises a viral DNA Binding and Dimerization domain (DBD) (Figure 1.3)[29,30].

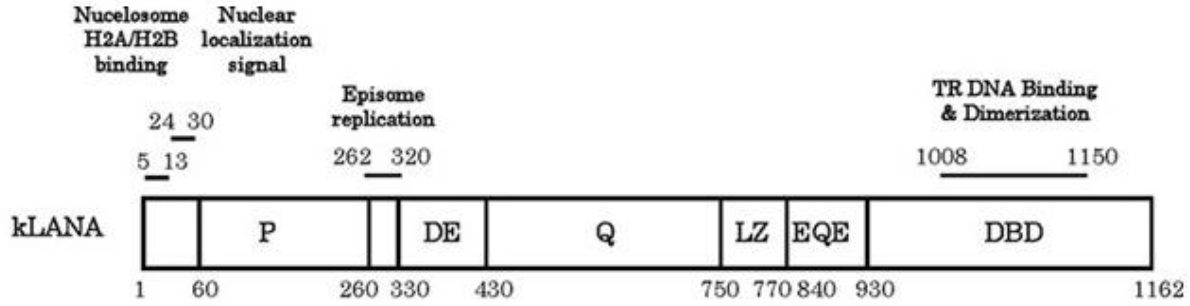

Figure 1.3 – Schematic representation of kLANA. Its structure can be divided into an N-terminal proline rich region (P), a glutamate-aspartate (DE), Glutamine (Q), glutamine-glutamate (EQE) and putative leucine zipper (LZ) central region, and a DNA Binding and Dimerization (DBD) region in the C-terminal. Adapted from Ponnusamy et al. (2015)[27].

1.3.1. Tethering of the KSHV genome to host chromosomes

kLANA is essential for the maintenance of the episome throughout the regular cell cycle, guaranteeing a stable copy number of the viral genome in daughter cells[22]. The protein is able to bind to the viral episome TRs through its C-terminal while simultaneously binding directly to the nucleosome of host chromosomes through its N-terminal, tethering the viral episome to the host chromosomes[17]. kLANA binds to specific sequences in TRs called LANA binding sites (LBS), of which three different ones (LBS 1, 2 and 3) are known in KSHV. Each LBS presents a different binding affinity to kLANA and only binds to a kLANA dimer which contains two recognition half-sites[22,30]. The dimerization occurs through the formation of a β-barrel composed of eight anti-parallel strands (four from each LANA molecule) flanked by three α-helices on each side[29]. The presence of the LBS sequences in tandem requires the further oligomerization of kLANA and cooperativity in the interaction to LBS[22,30]. N-terminal binding occurs directly to the surface of the nucleosome, which functions as a docking station. The hairpin formed by kLANA amino acid residues 5 to 13 can bind with high stability to the acidic patch formed by the histone H2A and histone H2B dimer (Figure 1.4)[31].

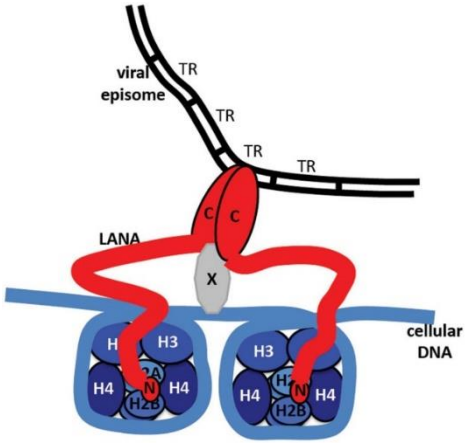

Figure 1.4 – Schematic representation of tethering of the viral episome to cell chromosome. kLANA's C-terminal dimerizes and binds to TRs and a putative (X) protein that interacts with the chromosome while the N-terminal binds directly to the nucleosome (H2A-H2B acidic patch)[22].

In addition to binding to chromosomal nucleosomes, kLANA is also able to interact in the same way with viral nucleosomes, establishing clusters of episomes. In the TR region of viral DNA, each TR contains three LBS close together and free from nucleosomes. In between sets of LBS, three to four nucleosomes bind to the viral DNA. Given this structure, kLANA binds directly to the DNA of one episome through its C-terminal while simultaneously binding to other episome nucleosomes through its N-terminal, tethering together several KSHV episomes and forming clusters of KSHV genomes[32].

1.3.2. DNA replication and episome segregation

The clustering of KSHV genomes is advantageous for replication[32], another mechanism in which kLANA plays a role. Replication of the viral DNA is necessary to maintain a stable number of copies of KSHV genome per cell[21]. This number varies according to the presenting form of the disease, with PEL cells showing between 50 and 100 copies per cell while KS cells contain approximately only one copy

per cell[8,21]. This suggests that KSHV recruits the DNA replication cell machinery in order to replicate its own genome only once per cell cycle during mitosis[33].

In latency, the origin of replication for the KSHV genome (ori-P) is found within the TRs, comprising LBS 1 and LBS 2 as well as a subsequent 32 bp GC-rich segment[33]. Additionally, the replicator element (RE) – a 31 bp sequence upstream from LBSs – is critical for the initiation of replication. The recruitment of the pre-replication complexes to the ori-P is dependent on kLANA and these include origin recognition complexes (ORCs), Cdc6, Cdt1 and mini-chromosomal maintenance proteins (MCMs). Further recruitment of the cellular replication machinery such as origin recognition complex proteins, Topoisomerase IIβ, replication protein A (RPA) and proliferating cell nuclear antigen (PCNA) is achieved in a coordinated manner in order to kick off the DNA replication[21,25]. Since at least two REs and their respective LBSs are needed for efficient maintenance of episomes, the spatial configuration of kLANA bound to TRs is critical for the assembly of the host machinery, giving rise to the characteristic kLANA speckles observed in KSHV-infected mitotic cells[29].

After DNA replication, the newly formed episomes must be segregated into the daughter cells' nuclei. This mechanism is not yet fully understood. However, it has been shown that the central region of kLANA, more specifically residues 33 to 194, plays an essential role. Potentially, these residues could be involved in the strengthening of N-terminal kLANA binding to nucleosomes, by interacting with chromatin in a different way. Another alternative role for this sequence could be during replication by maintaining contact with H2A and H2B when they lose contact with DNA or by ensuring they reattach when new nucleosomes are assembled[34]. As LANA also interacts with SSRP1, a member of the facilitating chromatin transcription complex (FACT) which is responsible for the disruption and reassembly of nucleosomes by destabilization of H2A/H2B dimers, it is interesting to speculate that this complex may be involved in segregation[17,34].

1.3.3. Chromatin modifications

kLANA's interactions with chromatin are not exclusively related with tethering of the viral episome to host chromosomes. Studies have demonstrated that kLANA is able to interact with both H3K9 methyltransferase SUV39H[35] and the H3K9 demethylase KDM3A[36] to regulate the transcription of lytic genes through epigenetic modifications. kLANA is also able to bind to the histone acetyltransferase CBP and histone deacetylase complex mSin3[37]. Additionally, kLANA mediates the recruitment of Polycomb Repressive Complexes (PRC1 and PRC2) to deposit H3K27me3 histone modifications on the KSHV genome. This is a sequential process in which kLANA interacts with PRC2 in order to methylate H3K27. Only after this modification is in place can PRC1 be recruited to the site, co-localizing with PRC2 and kLANA in LANA speckles[38].

Moreover, regarding H3K4me3 activating marks, it has been shown that kLANA interacts with and is responsible for the recruitment of one of the mammalian lysine methyltransferases (KMTs), the hSET1 complex, onto KSHV genome to activate latency promoters[37]. Preliminary results showed that kLANA is also able to interact with the MLL1 COMPASS complex, another KMT, recruiting it to TR DNA. The MLL1 COMPASS complex core proteins consist of the MLL1 catalytic enzyme sandwiched between the WDR5-RbBP5 subcomplex and the ASHL2 subunit, allowing for the interaction of the COMPASS

complex with the nucleosome (Figure 1.5.A)[39], with WDR5 essential for the formation and stability of this complex[40].

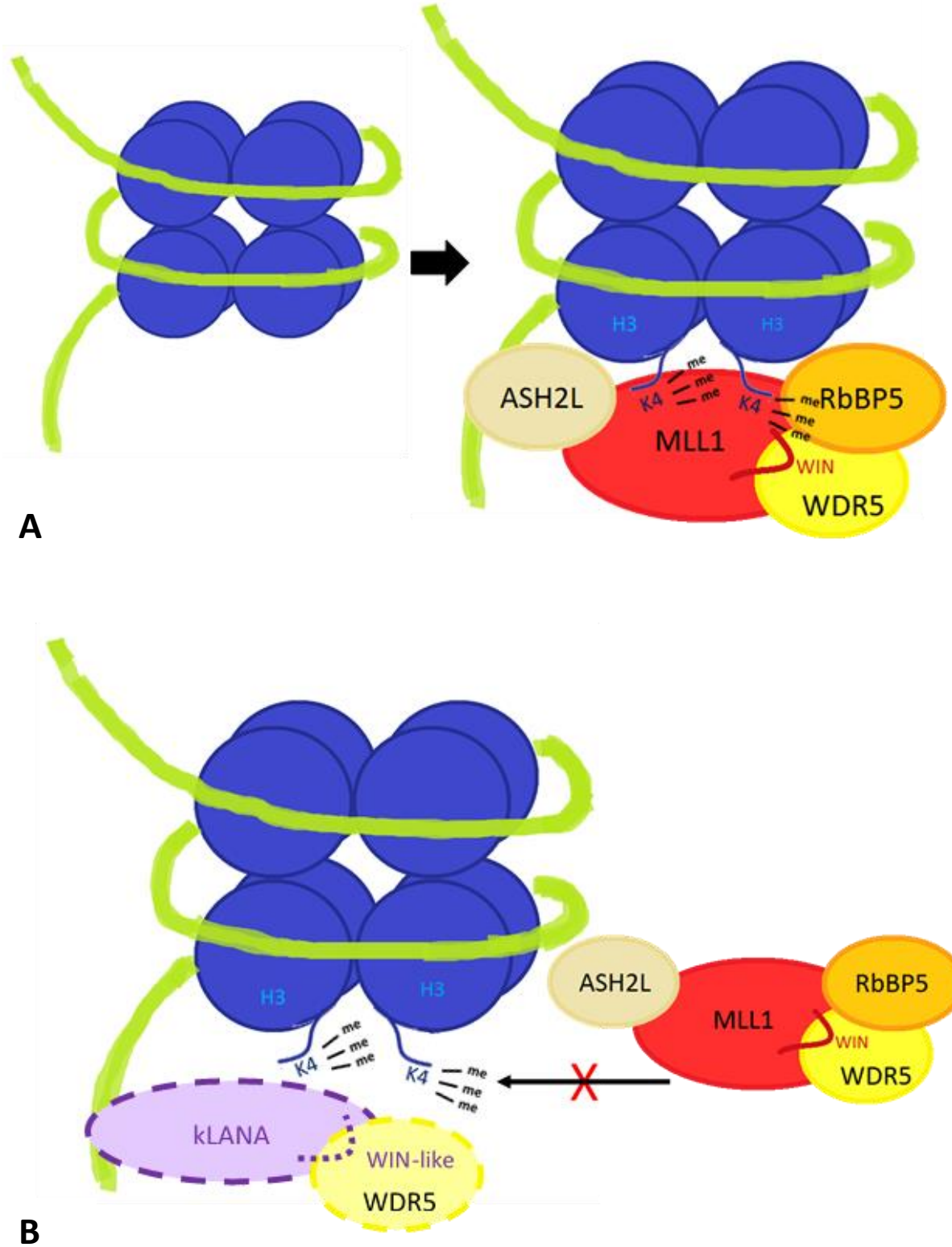

Figure 1.5 – Schematic representation of the mechanism of interaction between kLANA and the MLL1 COMPASS complex. A – Schematic representation of the nucleosome and the MLL1 COMPASS complex core, constituted by MLL1 catalytic enzyme, WDR5, RbBP5 and ASHL2, bound to the nucleosome for H3K4me deposition. MLL1 binds to WDR5 through the WIN motif. B – Schematic representation of the nucleosome and the potential interaction between kLANA and WDR5 through a WIN-like motif that prevents the MLL1 COMPASS complex from assembling and promoting H3K4me3 deposition.

At the beginning of *de novo* infection (8 hours p.i.), kLANA exists in low amounts leading to low H3K4me3 deposition. As kLANA expression increases by 16 hours p.i. high deposition of H3K4me3 is achieved. Then, as kLANA levels increase further, MLL1 activity is inhibited, H3K4me3 levels decrease due to demethylase activity. The inhibition of MLL1 catalytic activity is probably related to competition between MLL1 and kLANA to bind WDR5, an essential protein for MLL1 activity (unpublished results). WDR5 binds to MLL1 through the WDR5 interaction motif (WIN motif) and is critical for the KMT activity of MLL1[40,41]. The WIN motif is present in all MLL proteins and consists of 11 amino acid residues which include a conserved arginine essential for interaction between MLL and WDR5[42]. A WIN-like motif was found to exist in kLANA's N-terminal, thus suggesting competition between MLL1 and kLANA binding to WDR5 to be the mechanism of MLL1 inhibition (Figure 1.5.B). There is, however, another possibility that cannot be excluded at this point, where kLANA also interacts with MLL1 and can affect the KMT catalytic site directly. This interference with MLL1 activity is thought to be a mechanism of defence from Dnase1L3 activity, so that KSHV can be maintained in host cells (unpublished results). In the interest of uncovering the mechanisms of MLL1 KMT activity inhibition, it would be possible to introduce mutations in kLANA in the WIN-like motif to increase or decrease its affinity to WDR5 and observe the effects in the establishment of latency.

1.4. Animal model for the study of KSHV

The species specificity of KSHV introduces a massive obstacle to the study of the mechanisms of infection and pathogenesis of this virus *in vivo*, thus creating the need for a reliable animal model of this infection. Due to the fact that some of the main characteristics of gammaherpesviruses include their ability to establish latent infections in lymphocytes as well as induce lymphoproliferative disease and their close association with a variety of tumours[43], a gammaherpesvirus that can infect laboratory animals presents a potential model for the understanding of KSHV infection *in vivo*[44]. One such example is MHV-68[20,43,44].

1.4.1. MHV-68

MHV-68 was first isolated from a bank vole (*Myodes glareolus*) in Slovakia[45]. Later, it was also found in yellow-necked mice, shrews and wood mice, indicating a wide variety of hosts and high infection rates among northern Europe rodents[43,46]. In spite of the fact that it has not been identified in house mice, the natural counterpart of laboratory mice, it is able to infect these animals in both an acute and a persistent manner and does not present high pathogenicity or marked attenuation generally shown by herpesvirus in xenogeneic hosts, offering thus a unique and reasonable model to study pathogenesis[46,47].

Usually, infection of laboratory mice is performed by intranasal inoculation which first leads to an acute productive infection in the lungs that lasts for two weeks, with a peak around 7 days post inoculation and resolution at 10-12 days post inoculation, This is followed by a life-long persistent infection of lymphoid tissue which is characterized by a transient phase of splenomegaly that peaks at 2-3 weeks post inoculation followed by persistent latent infection of memory B-cells[43,46–48]. Latent infection has also been identified in epithelial cells, macrophages, and dendritic cells[49]. The pathology

in mice associated with MHV-68 infection is an infectious mononucleosis-like syndrome with lymphocyte activation[49].

The MHV-68 genome is highly similar to the KSHV genome, both in terms of structure, with a low GC % central region flanked by high GC % repetitive sequences, and organization, with blocks of co-linear and homologous ORFs interspaced with virus specific ORFs characteristic of gammaherpesvirus[43,50]. One of these ORFs is ORF 73, i.e. the MHV-68 homologue to kLANA, also known as mLANA[29].

1.4.2. mLANA

mLANA is a much smaller protein than kLANA, consisting of 314 amino acid residues. It resembles kLANA most especially in its C-terminal which also comprises a DNA binding and dimerization domain (DBD) structurally similar to kLANA's[29,51]. mLANA's N-terminal also contains a proline rich region (Q). The similarities end here since there is a notable absence of the glutamate, aspartate and glutamine rich central region that exists in kLANA which is responsible for mLANA's much smaller size (Figure 1.6)[29,49].

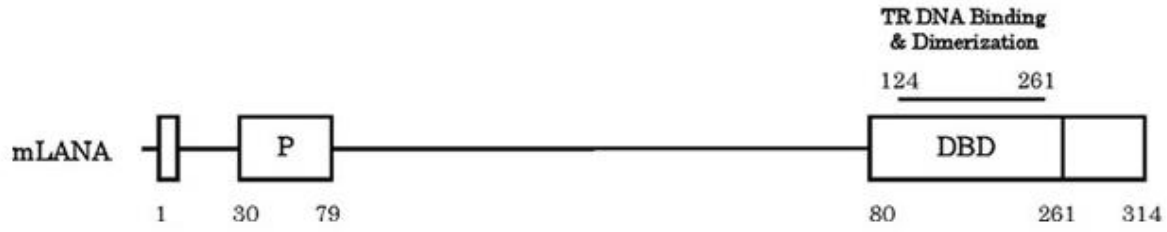

Figure 1.6 – Schematic representation of mLANA. N-terminal includes a proline rich region while the C-terminal comprises a DNA binding and dimerization domain (DBD) which are homologous to kLANA regions. Adapted from Ponnusamy et al. (2015)[27].

Despite the differences between LANAs, some of their functions remain conserved[51]. mLANA is able to tether episomes to host chromosomes, through binding to MHV-68 TRs during mitosis, ensuring the maintenance of viral genomes in daughter cells[49]. It also plays a role in replication of episome DNA through TRs[51]. Together, these corroborate the critical role of mLANA in the establishment and maintenance of latency[52].

Nonetheless, other functions are specific to either mLANA or kLANA. For example, mLANA promotes replication through the inhibition of the apoptotic response mediated by p53 and the recruitment of the heat shock cognate protein 70 (Hsc70). Contrastingly, kLANA actively represses lytic activation through repression of RTA transcription, a function not observed for mLANA[51]. Additionally, it has been determined that, although both proteins form dimers in order to bind to viral TR DNA, kLANA forms intrinsically bent oligomers while mLANA arranges in a more strict linear way[29].

1.4.3. Chimera viruses

Given the similarities between mLANA and kLANA, especially in the DBD, it was proposed that their functions might be interchangeable, allowing for the development of an animal model for *in vivo* studies of kLANA[48,51,53]. mLANA was found to be able to bind to TRs from KSHV and maintain plasmids that contained these sequences through cell division. Similarly, kLANA supported episome persistence of

plasmids containing TRs from MHV-68[53]. Considering this, chimera viruses were constructed by substituting the mLANA gene with kLANA in the MHV-68 genome[51,53]. Chimera virus managed to establish long-term latency in mice, although a modestly attenuated phenotype was observed[51,53]. This was the result of less infected cells, while the number of episomes per cell was equivalent when comparing the wild-type virus to the chimera one[48,53]. Since kLANA represses ORF50 expression, something mLANA is not able to do[51], this result is possibly connected with low lytic reactivation during the initial stages of latency establishment[53].

Together, these results present a novel model for the study of kLANA *in vivo*, from understanding the mechanisms for infection outcome related to kLANA to testing potential small molecule drugs that target kLANA[48,51,53]. These chimera viruses are also an important tool to test the effects of mutations in kLANA on the life cycle of the virus *in vivo*, whether lytic or latent infection is of interest.

The construction of chimera viruses and potential mutations of interest usually involves the use of Bacterial Artificial Chromosomes (BACs), since the genomes of herpesvirus are too large to clone into plasmids or cosmids and Yeast Artificial Chromosomes (YACs) are less stable and more likely to suffer rearrangements or contaminations with yeast sequences. To construct a viral BAC, a BAC vector must be inserted into the viral genome. There are viral BACs for most of the human herpesvirus as well as for some animal viruses that are used as animal models[54]. This is the case for MHV-68, which was cloned as a BAC in *Escherichia coli*[55]. BAC vectors, and thus, viral BACs, include an origin of replication, genes necessary for BAC replication, genes that control the rate of replication to control the number of BAC copies in a cell, an antibiotic resistance gene and a selection marker. Additionally, two loxP sites at the ends of the BAC sequence are generally included in order to remove BAC sequences when generating recombinant viruses using Cre recombinase[54,55]. Therefore, viral BACs can be maintained in *E. coli* and be transfected into eukaryotic cells to obtain recombinant viruses. Mutagenesis can be performed through homologous recombination, transposon mutagenesis or site directed mutagenesis (ET cloning)[55].

1.5. Aim of the project

The importance of LANA in the establishment of persistent KSHV infection and viral genome maintenance, as well as its tumorigenic properties have been well documented. However, the mechanisms behind this importance are still unclear, making the study of this protein essential for the development of anti-KSHV therapies.

Previous studies have shown that kLANA is able to interact with histone modification complexes to affect chromatin modifications, including methylation and acetylation of viral histones[35–38]. Preliminary results showed kLANA interacts with the HMT MLL1 complex through kLANA's WIN-like motif and indicate that LANA regulated MLL1 H3K4me3 deposition in TR DNA through competitive inhibition of WDR5 interaction. Moreover, a novel antiviral host mechanism mediated by a nuclear endonuclease was identified, as endonuclease mediated viral DNA degradation correlated with TR levels of H3K4me3. These results suggest that understanding the mechanisms behind this interaction will give important insights into virus persistence, hence its putative pharmacological control.

The aim of this project was to evaluate the relevance of kLANA's WIN-like motif and, thus, the interaction between WDR5 and kLANA, in the establishment of persistent infection *in vivo* through the use of recombinant viruses with mutations in kLANA that either increase or decrease its affinity towards WDR5. These recombinant viruses would then be used to infect mice in order to assess their impact on latency.

CHAPTER TWO:

MATERIALS AND METHODS

2.1. Materials

2.1.1. Cell lines

NIH-T3T-CRE (Cre) cells[56], fibroblasts that express Cre recombinase, a tyrosine recombinase from bacteriophage P1, were cultured in Dulbecco's Modified Eagle Medium (DMEM) supplemented with 10 % Foetal Bovine Serum (FBS), glutamine 2 mM, penicillin 100 U/mL, and streptomycin 100 U/mL. Baby hamster kidney fibroblast (BHK-21) cells were maintained in Glasgow's Minimum Essential Medium (GMEM) supplemented as described before with the addition of 10 % Tryptose Phosphate Broth (TPB). Cells were cultured in an incubator at 37 °C and in 5 % CO_2.

2.1.2. Viruses

v.WT was derived from a genomic BAC and it was kindly offered by Dr Heiko Adler and Dr Ulrich Koszinowski. This virus is essentially a MHV-68 clone G2.4, that was isolated from virus grown in BHK-21 cells, but contains a single loxP site[55,57,58].

v.kLANA, v.AARA I, v.AARA II and v.PAA were reconstituted from BAC DNA that were previously engineered by Dr Andreia Mósca in the host lab. Each BAC included the MHV-68 genome where mLANA was substituted for wild-type or mutated kLANA and its 5'UTR, the BAC vector, a guanosine phosphoribosyl transferase (GPT) gene, a green fluorescent protein (GFP) gene and two *loxP* sites[55,58]. v.kLANA encodes for the virus expressing the wild-type kLANA. v.AARA I and II are two independently reconstituted viruses for this mutation (22SCRK25→22AARA25). v.PAA encodes for the recombinant virus expressing the mutated kLANA 23CRK25→23PAA25.

2.1.3. Mice

Six-week-old female BALB/cByJ mice were purchased from Charles Rivers Laboratories, France. Mice were housed and subjected to experimental procedures at Instituto de Medicina Molecular João Lobo Antunes rodent facility, Lisbon, Portugal.

2.1.4. Antibodies

Primary antibodies used included: anti-kLANA rat monoclonal antibody (LN53, ABI Sciences) at 1:500 dilution, anti-mLANA mouse antibody 6A3 IgG1 (hybridoma supernatant)[59] at 1:10 dilution, anti-eGFP mouse monoclonal antibody (Clontech) at 1:1000 dilution, and anti-actin rabbit polyclonal antibody (Sigma) at 1:1000 dilution.

Secondary antibodies used were conjugated with horse radish peroxidase (HRP) and included anti-rabbit, anti-mouse, and anti-rat antibodies (Jackson Immunoresearch) at 1:5000 dilution.

2.1.5. Buffers and solutions

PBS – Phospate Buffered Saline 1 M

PBS-tween – 0.05 % Tween-20 in PBS

Blocking solution – 0.05 g/mL non-fat powder milk in PBS-tween

Laemmli Buffer – 100 mM Tris-HCl pH 6.8, 20 % glycerol, 4 %SDS, 10 % β-mercaptoethanol, 0.1 % bromophenol blue

Lysis Buffer for Protein extraction (LBP) – 150 mM NaCl, 10 mM Tris-HCl pH 7.4, 1 mM Na_3VO_4, 1 mM NaF, complete protease inhibitors cocktail (Roche), 10 % Triton X-100

Lysis Buffer for DNA extraction (LBD) – 10 mM Tris-HCl, 3 mM $MgCl_2$, 50 mM KCl, 0.45 % NP-40, 0.45 % Tween-20, 0.5 mg/mL Proteinase K

Red Blood Cells Lysis Buffer (RBC) - 154 mM NH_4Cl, 14 mM $NaHCO_3$, 1 mM EDTA pH 7.3

Electrophoresis Buffer (TGS) – 25 mM Tris, 192 mM glycine and 0.1 % sodium dodecyl sulphate (SDS)

Transference Buffer (TG) – 25 mM Tris, 192 mM glycine, 20 % methanol, 0.037 % SDS

Stripping solution – 62.5 mM Tris HCl pH 6.8, 2 % SDS, 100 mM β-mercaptoethanol

2 % FBS/PBS – 2 % Foetal Bovine Serum in PBS

2.2. Methods

2.2.1. Virus synthesis

2.2.1.1. Virus reconstitution from BAC DNA

BHK-21 cells were seeded at $1x10^6$ cells per 6 cm dish and incubated for one day at 37 °C and in 5 % CO_2. BAC DNA was transfected into cells using X-tremeGENE HP (Roche Applied Science) with a ratio of 1 µg of DNA to 2 µL of reagent. Cells were incubated for three to four days, depending on the number and size of plaques observed, and scrapped into the medium and stored at -80 °C.

2.2.1.2. Removal of BAC sequences

Cre cells were seeded at $1.75x10^5$ cells per well in 6-well plates and incubated one day before infection. Infection was achieved by adding different amounts of reconstituted viral particles to the cells which were then incubated for three to four days. Then, GFP expression was used as a marker for effective removal of BAC sequences. Cells were observed under a fluorescence microscope. The presence of GFP indicated another passage through Cre cells was needed. The wells with the better ratio of cytopathic effect (CPE) to fluorescence intensity, i.e. more CPE to less fluorescence, were

chosen to scrape and re-infect Cre cells. In the absence of fluorescence, cells were scrapped into the medium and stored at -80 °C.

2.2.1.3. Virus titration

Viral titres were determined as plaque forming units per millilitre (PFU/mL) using the plaque assay method[60]. The method is based on the incubation of a confluent cell monolayer with viral particles and counting of the plaques formed after a set period of time. Plaques are empty spaces in the monolayer that result from cell lysis. In brief, ten-fold serial dilutions of viral sample were made at an inoculum of 900 µL. For titration of viral stocks, dilutions 10^{-3} to 10^{-8} were plated while for the BAC- (viral suspensions without BAC sequences) recovered from Cre cells dilutions 10^{-1} to 10^{-6} were plated. The viral dilutions were incubated with $2x10^5$ cells for one hour at room temperature under constant rocking. 2 mL of media were added and the mixture was poured onto 6-well plates. After incubation for four days, cells were fixed with 4 % formaldehyde (in PBS) for 10 minutes and stained with 0.1 % toluidine blue for 5 minutes. PFUs were counted with a plate microscope. Titres were calculated considering the dilution counted, the inoculum of virus (in mL) and PFUs counted, according to Equation 1.

$$Titre = average\ number\ of\ plaques \times \frac{1}{dilution} \times \frac{1}{inoculum} \quad (1)$$

2.2.1.4. Viral stock preparation

Viral stocks were prepared by infecting BHK-21 cells with an MOI (multiplicity of infection, i.e., the ratio between viral PFUs and the number of cells) of 0.002. After incubation on a 5 % CO_2 atmosphere for three to four days, until approximately 50 % of cells presented CPE, cells were scraped into the medium and centrifuged at 435 *g* at 4 °C for 5 minutes. The pellet was resuspended in supplemented GMEM and stored at -80 °C, constituting the cell working stock (CWS). The supernatant was then centrifuged at 15000 *g*, for two hours at 4 °C. The pellet was resuspended in supplemented GMEM and stored at -80 °C, constituting the working stock media (WSM) to be used in further experiments.

2.2.2. *In vitro* assays

2.2.2.1. Protein extraction

BHK-21 cells, seeded the day before at $1x10^5$ cells per well in 24-well plates, were infected with an MOI of 3 with each recombinant virus as well as v.WT. Cells were incubated for two hours, after which the inoculum was removed and cells were washed with warm media. Cells were incubated for another four hours after media was added. Cells were then washed twice with ice-cold PBS and disrupted with LBP. Lysates were cleared by centrifugation at 18 000 *g* and prepared for SDS-PAGE with 2x Laemmlli Buffer.

2.2.2.2. SDS-PAGE

Proteins were separated by sodium dodecyl sulphate-polyacrylamide gel electrophoresis (SDS-PAGE) using a stacking gel of 5 % polyacrylamide (polyacrylamide mix (acrylamide/bis-acrylamide 37.5:1, Bio-Rad), 0.065 M Tris HCl (pH 6.8), 0.1 % SDS, 0.1 % ammonium persulphate (APS), 0.04 % tetramethylethylenediamine (TEMED)) and a resolving gel of 10 % polyacrylamide (polyacrylamide mix, 0.390 M Tris HCl (pH 8.8), 0.1 % SDS, 0.1 % APS, 0.01 % TEMED) in 1.5 mm mini-slab gels (Mini-

PROTEAN II Electrophoresis System, Bio-Rad). Before application of 50 µL per sample into the gel, protein samples were heated to 95 °C for 3 min. The gel was run at 180 V for approximately one hour in TGS.

2.2.2.3. Western Blot

Proteins were transferred to a nitrocellulose membrane in TG overnight at 100 mA, 4 °C. To ensure proteins were successfully transferred, the membrane was incubated with Ponceau S dye (Sigma) for 10 minutes. The dye was then removed by washing twice with PBS-Tween. The membrane was cut into three pieces taking into account the molecular weights of the proteins probed. Membranes were incubated for 30 minutes at 10 rpm, at room temperature (RT) with blocking solution, to reduce non-specific binding of antibodies to the membranes, and then washed twice with PBS-Tween, at 10 rpm RT. Then, membranes were incubated with the corresponding primary antibody (described in section 2.1.4) either for one hour, at 10 rpm, RT, or overnight, at 10 rpm, 4 °C, and washed three times with PBS-Tween for five minutes. Afterwards, membranes were incubated with the corresponding secondary antibodies for 30 minutes, at 10 rpm, RT, and washed three times with PBS-Tween for five minutes. Protein bands were detected by chemiluminescence using SuperSignal™ West Pico Chemiluminescent Substrate (Thermo Scientific), according to manufacturer's instructions, in a Chemidoc XRS+ (Bio-Rad) or Amersham 680 RGB (GE Healthcare). In order to re-probe membranes with different antibodies, membranes were stripped by incubation at 55 °C in stripping solution for 30 minutes, washed 4 times with PBS-Tween, incubated with blocking solution at RT for 10 minutes and re-probed.

2.2.2.4. Multi-Step Growth Curve

BHK-21 cells, seeded the day before at $5x10^4$ cells per well in 24-well plates, were infected with an MOI of 0.01 with each virus and incubated for one hour at 37 °C. After, the inoculum was removed and cells were washed twice with PBS. Media was added to each well and cells were incubated at 37 °C. Cells were harvested at 6 timepoints – immediately after addition of media (0 h), after 24, 48, 72, 96 or 120 hours post infection (h.p.i.) – and stored at -80 °C. Titres for each timepoint and virus were determined as described in section 2.2.1.3..

2.2.3. Animal experiments

2.2.3.1. Ethics statement

This study was performed in accordance with the Portuguese Official Veterinary Directorate (Portaria 1005/92), European Guideline 86/609/EEC, and Federation of European Laboratory Animal Science Associations guidelines on laboratory animal welfare. It was approved by the iMM Animal Ethics Committee and by the Portuguese official veterinary department for welfare licensing (Direção Geral da Alimentação e Veterinária).

2.2.3.2. Mice infection

Female BJAB/c mice (Charles River Laboratories) were anesthetized with a low dose of isoflurane and infected intranasally with 10^4 PFUs of each virus (v.kLANA, v.AARA I, v.AARA.II, v-PAA) in 20 µL PBS. Each of the four experimental groups was composed of 4 to 6 animals. Mice were sacrificed with an overdose of isoflurane at three different timepoints – 7, 14 and 21 days post-infection (d.p.i.). At 7

d.p.i. lungs were harvested into 5 mL of GMEM and processed as described in section 2.2.3.3. while at 14 and 21 d.p.i. spleens were harvested into 5 mL of GMEM and processed as described in section 2.2.3.4..

2.2.3.3. Lytic infection in the lungs

Lungs harvested from mice at 7 d.p.i. were frozen at -80 °C for at least an hour, freeze-thawed and homogenized in glass homogenizers and frozen again overnight. Homogenates were freeze-thawed, vortexed and centrifuged for 1 minute at 300 *g* in order to remove lung debris that could affect the BHK-21 monolayer. The supernatant was then titrated as described in section 2.2.1.3..

2.2.3.4. Infectious centre assay

Spleens harvested from mice at 14 or 21 d.p.i. were processed into single cell suspensions using a 100 µm cell strainer and a syringe. Cells were centrifuged at 300 *g* for 5 minutes at 4 °C. The pellet was resuspended in 1 mL of RBC and incubated on ice for 5 minutes to remove erythrocytes. 5 mL of GMEM were added and cells were centrifuged at 300 *g* for 5 minutes at 4 °C. The pellet was resuspended in 5 mL of GMEM to obtain a splenocyte suspension. 10-fold dilutions of splenocytes were prepared in GMEM and co-cultured in 6 cm dishes with 4-5x10^5 BHK-21 cells per dish. Cells were incubated for 5 days.

Splenocyte suspensions were also screened for preformed viruses. Suspensions were frozen at -80 °C in order to disrupt cells. After thawing, 500 µL of each suspension were added to 4-5x10^5 BHK-21 cells in 6 cm dishes and media was added up to 5 mL. Cells were incubated for 4 days.

In both assays, cells were fixed and stained, and viral titres were calculated as described in section 2.2.1.3..

2.2.3.5. Limiting dilution assay coupled with real-time PCR (qPCR)

The frequency of viral DNA positive cells was assessed per experimental group. A pool of splenocytes per experimental group was prepared using 250 µL of each splenocyte suspension described in section 2.2.3.4.. Cells were centrifuged at 200 *g*, for 5 minutes at 4 °C. The supernatant was discarded and the pellet resuspended in 2 % FBS/PBS. Cells were centrifuged again at 200 *g*, for 5 minutes at 4 °C. The supernatant was discarded and cells were resuspended in 2 % FBS/PBS. The cell suspension was cleared by passing through a 40 µm cell strainer. Each pool was counted in order to prepare a suspension of 2x10^6 cells/100 µL in 2 % FBS/PBS. Serial 2-fold dilutions were prepared in 2 % FBS/PBS. 10 µL of LBD were distributed to PCR strip tubes and 5 µL of dilutions were added to each tube to obtain 8 replicates per dilution. Strips were incubated at 37 °C overnight. Proteinase K was inactivated by heating cell lysates to 95 °C for five minutes. Lysates were stored at -20 °C.

Samples were analysed by real-time PCR (qPCR) in a Rotor Gene 6000 (Corbett Life Science), according to the manufacturer's instructions using a fluorescent Taqman probe (M9-T) (Alfagene) and primers (forward, M9-F, and reverse, M9-R) specific for the MHV-68 M9 gene (Table 2.1). PCR reactions were carried out in a total volume of 25 µL containing 2.5 µL of sample, 200 nM of each primer, 300 nM of the M9-T probe, 1x Platinum qPCR SuperMix-UDG (Invitrogen), 5 mM of MgCl2 and nuclease-free

water. A negative control (nuclease free water) and a positive control (known copy numbers of pGBT9-M9, a plasmid containing the M9 gene) were used in each run. The PCR program consisted in: a first hold at 50 °C for 2 minutes, a second hold at 95 °C for 10 minutes, a cycling step repeated 50 times consisting of heating to 95 °C for 15 seconds followed by 30 seconds at 60 °C, during which fluorescence was acquired using the green channel with a gain of 5.33. Results were analysed using the RotorGene 6000 series (1.7) software. Each sample was scored as positive or negative in comparison with the controls used.

Table 2.1. – Probe and primer sequences for the detection of the MHV-68 M9 gene.

Probe/Primer	Oligonucleotide sequence (5'- 3')
M9-T	6-FAM-CTTCTGTTGATCTTCC-MGB[a]
M9-F	CAGGCCTCCCTCCCTTTG
M9-R	GCCACGGTGGCCCTCTA

[a] Oligonucleotide with a fluorophore (6-FAM) and quencher (MGB) covalently attached to its 5'- and 3'-ends, respectively.

The frequency of viral DNA positive cells was determined according to the single-hit Poisson model (SHPM) by maximum likelihood estimation[61]. The model assumes that one cell of one cell subset is necessary and sufficient to generate a positive response. This method consists in modelling the limiting dilution data according to the linear log-log regression model.

2.2.4. Statistical Analysis

Statistical analysis was performed using GraphPad Prism 8.4.3 software, using the nonparametric two-tailed Mann-Whitney test or the one-way analysis of variance (ANOVA; Kruskal-Wallis test), as appropriate. For the limiting dilution assays, 95% confidence intervals were determined as described by Marques et al. (2003)[62].

CHAPTER THREE:

RESULTS

3.1. Generation of MHV-68 recombinant viruses

It has been recently discovered that kLANA's N-terminal includes a small motif similar to the WDR5 interaction (WIN) motif of the histone methyltransferase MLL1. This motif allows for kLANA to interact with WDR5 and disrupt the formation of the MLL1 complex. This complex is responsible for the tri-methylation of viral TR histones which has been correlated with viral DNA degradation. kLANA's ability to disrupt MLL1 activity prevents this degradation and allows for the establishment of infection. In order to understand how the mechanisms behind this interaction affect the establishment of latency *in vivo*, two recombinant viruses were reconstituted from BAC DNA that was previously engineered to introduce mutations in kLANA's WIN-like motif (Table 3.1). One mutation was engineered in order to increase the affinity between kLANA and WDR5 by increasing the similarity between kLANA's WIN-like motif and MLL1's WIN (22SCRK25→22AARA25). The other was engineered to decrease the affinity between kLANA and WDR5 through the removal of a critical arginine for the interaction (23CRK25→23PAA25).

Table 3.1 - WIN and WIN-like motifs from MLL1, kLANA and mutated kLANAs. The conserved arginine critical for interaction with WDR5 is highlighted in blue.

Protein	WIN or WIN-like motif					
MLL1	**G**	**S**	**A**	**R**	**A**	**E**
kLANA	**G**	**S**	**C**	**R**	**K**	**R**
kLANA 22SCRK25→22AARA25	**G**	**A**	**A**	**R**	**A**	**R**
kLANA 23CRK25→23PAA25	**G**	**S**	**P**	**A**	**A**	**R**

Bacterial artificial chromosomes (BACs) coding for the MHV-68 genome where mLANA was substituted for kLANA, mutant and non-mutant, were transfected into BHK-21 cells in order to reconstitute the viruses. Reconstituted viruses consisted of one control virus with non-mutant kLANA (v.kLANA), two independently derived mutants for $kLANA_{22SCRK25→22AARA25}$ (v.AARA I and v.AARA II) and one independent mutant for $kLANA_{23CRK25→23PAA25}$ (v.PAA). The BAC cassette in reconstituted viruses, external to the MHV-68 genome and flanked by *lox*P sites, was removed using a Cre-lox system by infecting cells expressing Cre recombinase with the reconstituted viruses. Constantes de afinidade

3.2. Production of high titre viral stocks

Viral stocks to be used in this study were produced in BHK-21 fibroblasts and titrated to determine the viral particle concentration (Table 3.2). All titre values were in the range of those typically obtained in the laboratory (>10^6 PFUs/mL).

Table 3.2 – Viral stock titration. Viral titres obtained are presented in PFUs/mL.

Virus	Viral titre (PFUs/mL)
v.kLANA	$5.5x10^6$
v.AARA I	$4.2x10^7$
v.AARA II	$1.1x10^7$
v.PAA	$3.4x10^8$

3.3. Recombinant viruses express WIN-like motif mutant kLANA *in vitro*

To assess whether the introduction of mutations in kLANA WIN-like motif led to unexpected problems in the expression of this protein, BHK-21 fibroblasts were infected with the generated viruses as well as the WT virus (v.WT) with an MOI of 3 for 6 hours. Uninfected cells were used as a cell control. Then, total lysates from infected cells were separated by SDS-PAGE and the viral proteins of interest (kLANA and mLANA) as well as the cellular control (actin) were detected by Western Blot using specific antibodies.

kLANA was detected using a commercially available antibody, LN53, which recognizes the repetitive glutamic motifs EQEQE found in the internal glutamate and glutamine repeat region (EQE). As expected, since the mutations introduced in kLANA were substitutions, all kLANA proteins were detected at around 250 kDa, with no differences in molecular weight between mutant and non-mutant kLANA (Figure 3.1, top panel). Additionally, several bands can be observed for kLANA, which represent its different isoforms, the result of noncanonical translation initiation and an alternative poly adenylation signal[63,64]. For v.kLANA, kLANA expression is lower than that observed for the other viruses (Figure 3.1, lane 3). However, actin (≈ 42 kDa), the sample loading control, also showed lower expression, suggesting all proteins in this sample were reduced, thus, there were no issues with kLANA expression. For all other lanes, including the mock sample using only uninfected cells, actin levels were similar (Figure 3.1, bottom panel). Although v.AARA I also presented lower kLANA expression (Figure 3.1), this can be explained as a momentary lowered expression, since the independently derived mutant did not present lowered expression, thus the lower levels were not a result of the introduced mutation. mLANA, with a molecular weight of approximately 50 kDa, was only detected in the v.WT, as expected (Figure 3.1, middle panel). Therefore, mLANA substitution for kLANA was successfully performed in all chimeric viruses. No viral proteins were detected in the mock sample as cells were not infected (Figure 3.1, lane 1).

3.4. WIN-like motif mutations in kLANA do not affect growth kinetics *in vitro*

It has been demonstrated that LANA is not required for effective lytic replication *in vitro* or *in vivo*[52]. However, it is important to confirm that the mutations introduced in this protein do not affect the lytic phase of the virus, since the objective is to analyse the influence of these mutations in the latent phase. As such, a multi-step growth curve was executed. BHK-21 cells were infected with a low MOI (0.01) and the viral titres at 6 different time points were determined by plaque assay.

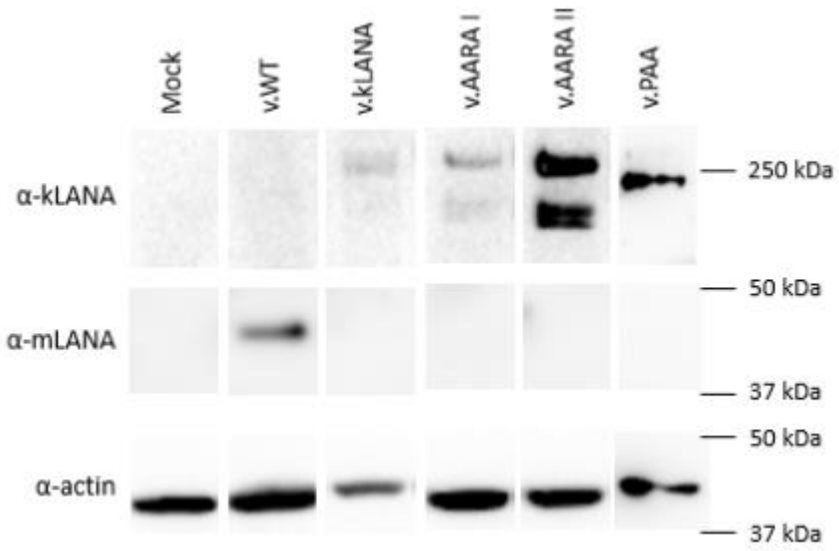

Figure 3.1 – Western Blot analysis of infected total cell lysates. BHK-21 cells were infected with v.WT and v.kLANA (lanes 2 and 3) as controls and the mutant recombinant viruses v.AARA I, v.AARA II and v.PAA (lanes 4, 5 and 6) at an MOI of 3 for 6 hours. A mock sample with uninfected cells was used as control (lane 1). Approximate molecular weights (kDa) are presented on the right.

Mutants displayed similar growth to v.WT and v.kLANA (Figure 3.2). Higher values for v.PAA on most time points were probably due to a higher initial inoculum. At 72, 96 and 120 h.p.i. there is a higher variability between viruses, which has been observed previously in the lab. Differences observed were not statistically significant (one-way non-parametric ANOVA WSC).

These results are in accordance with previous work in which mLANA was exchanged for kLANA. This alteration lead to no significant difference in growth kinetics *in vitro* between the WT virus and the chimeric virus[53]. Mutations in kLANA also presented no significant alterations in the lytic phase *in vitro* in previous works in the laboratory.

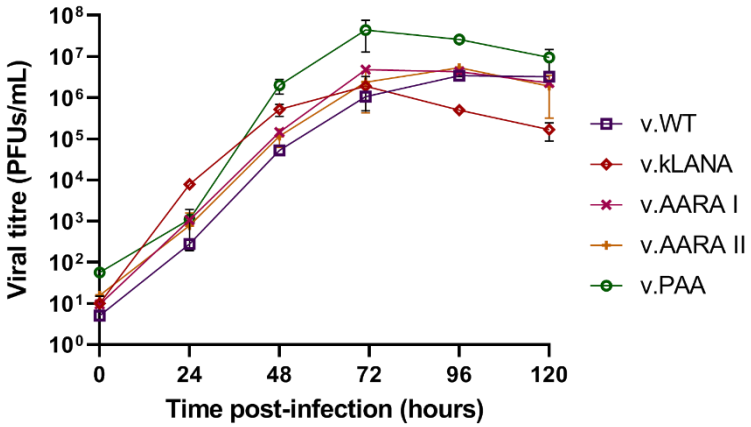

Figure 3.2 – Multi-step growth curves for WT and chimeric viruses. BHK-21 cells were infected with v.WT and v.kLANA as controls and recombinant viruses v.AARA I, v.AARA II and v.PAA at a low MOI (0.01). Cells were harvested at the presented time points (0, 24, 48, 72, 96 and 120 hours post-infection) and viral titres at each time point were determined by the suspension plaque assay. Time 0 indicates input virus after washing inoculum. No significant differences were identified between viruses (one-way non-parametric ANOVA Kruskal-Wallis test).

3.5. Mutated WIN-like motif kLANA recombinant viruses show normal lytic infection levels in the lungs

After intranasal infection, MHV-68 undergoes acute lytic infection in the lungs that peaks around 7 d.p.i. and is resolved by 10 to 12 d.p.i., involving the production and release of viral particles from alveolar epithelial cells[43]. In order to assess lytic infection *in vivo*, lungs from Balb/c mice infected intranasally with 10^4 PFUs and sacrificed at 7 d.p.i. were titrated by plaque assay after being homogenized and frozen so that progeny virions are released. The assay allows for the concentration of viral particles in the lungs to be determined through the infection of BHK-21 cells and formation of viral plaques (plaque assay).

Previous studies have shown that the growth kinetics of v.kLANA are similar to MHV-68 and that, despite slightly lower viral titres in the lungs for v.kLANA, those differences are not statistically significant[48,53]. As expected, since kLANA mutations were engineered to cause alterations in the latent phase, there were no significant differences between experimental groups in lung titres at 7 d.p.i. (Figure 3.3). The titres for v.AARA I were slightly lower than those of the other viruses. However, since the independently derived mutant did not present lowered titres, this result was attributed to experimental variability and not the engineered mutation. Therefore, these results indicate the mutations introduced in kLANA do not affect the lytic phase of infection and viruses were able to efficiently establish infection in the lungs.

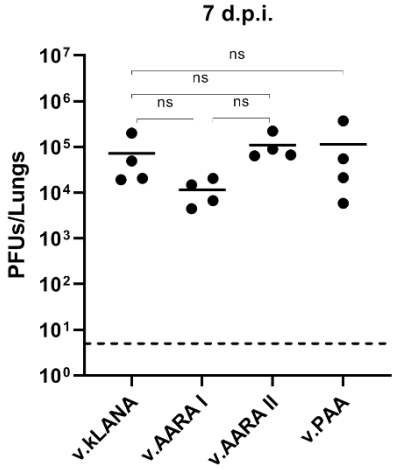

Figure 3.3 – Quantification of lytic infection in the lungs (PFUs/mL). Balb/c mice were inoculated intranasally with 10^4 PFUs in 20 µL of PBS of v.kLANA, v.AARA I, v.AARA II and v.PAA. Mice were sacrificed at 7 d.p.i. and lungs were harvested. Infectious viruses in the lungs were titrated by plaque assay. Each point represents the titre in the lungs of individual mice, each experimental group consisting of 4 mice. Bars indicate the mean of titres in each experimental group. The dashed line represents the limit of detection of the plaque assay. There was no significant difference between groups (p-value>0.05, Mann-Whitney test).

3.6. Impairing the interaction between kLANA and the MLL1 complex leads to diminished latency levels

LANA is essential for the establishment of latency in both MHV-68 and KSHV[52]. Previous studies have shown that mLANA can be exchanged for kLANA in MHV-68 while maintaining the virus' ability to establish persistent infection in the spleen, although at lower levels than the WT MHV-68[51,53]. Persistent infection reaches its peak at 14 d.p.i., rapidly decreasing after to levels that remain stable through life[62].

In order to assess latent infection in the spleen, an infectious centre assay, or *ex vivo* reactivation assay, was performed. The assay is based on the co-culture of splenocytes from infected mice with permissive BHK-21 cells. In these conditions, latent virus present in the splenocytes reactivates, infects BHK-21 cells and leads to the formation of viral plaques that can be counted in order to obtain a viral titre. Afterwards, since already formed viruses can also form viral plaques, splenocyte suspensions are frozen and thawed to release preformed viral particles. When cultured with BHK-21 cells, viral plaques form and viral titres are determined per spleen. The absence of plaques in this second step indicates virus titres from the first step are the result of latent virus only. In this study, Balb/c mice were inoculated with 10^4 PFUs of each virus and sacrificed at 14 and 21 d.p.i. for spleen removal and processing.

As expected, no pre-formed viruses were detected either at 14 or 21 d.p.i. (Figure 3.4, open circles), showing that the infection in the spleen was merely latent. v.kLANA was able to establish latent infection in the spleen and viral titres are higher at 14 (Figure 3.4.A) than 21 d.p.i. (Figure 3.4.B) similar to those already described[48,53]. Independent mutants v.AARA I and v.AARA II show similar viral titres to v.kLANA at both time points (Figure 3.4). There is, however, accentuated heterogeneity for v.AARA I at 14 d.p.i. (Figure 3.4.A), which means this time point should be repeated to confirm these results.

At 14 d.p.i. v.PAA presents slightly lower titres than v.kLANA, although they are not statistically significant ((Figure 3.4.A). There is also high variability among the experimental group. Therefore, this time point should also be repeated for clearer results. At 21 d.p.i. v.PAA cannot be detected (Figure 3.4.B), indicating this mutation resulted in reduced persistent infection.

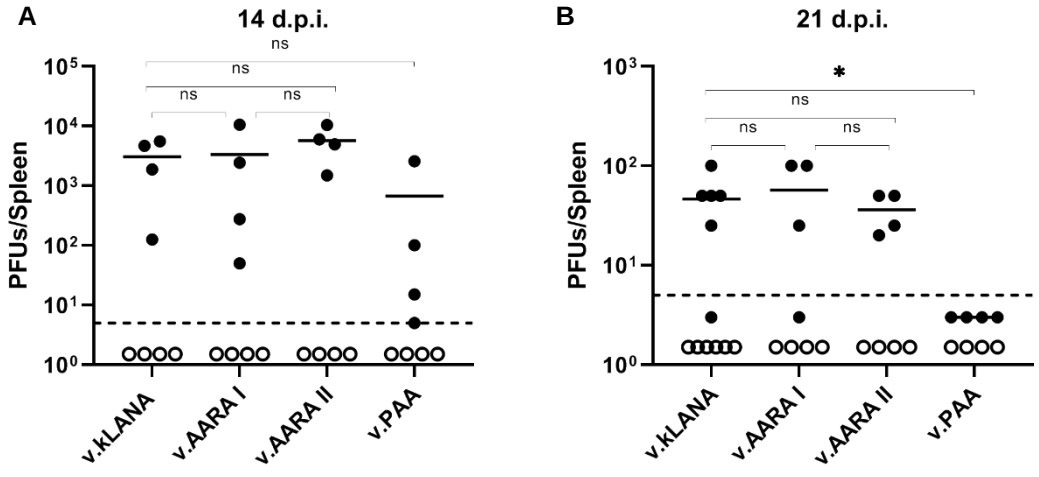

Figure 3.4 – Quantification of latent infection in the spleen (PFUs/spleen). Balb/c mice were inoculated intranasally with 10^4 PFUs in 20 µL of PBS of v.kLANA, v.AARA I, v.AARA II and v.PAA. Mice were sacrificed at (A) 14 and (B) 21 d.p.i. and spleens were harvested. Reactivating virus titres (closed circles) and pre-formed infectious virus titres (open circles) were determined by the infection centre. Circles represent individual mice. Bars indicate the mean in the experimental group, composed of 4 to 6 mice. The dashed line represents the limit of detection of the technique used. At 14 d.p.i. there was no significant difference between groups (p-value>0.05, Mann-Whitney test). At 21 d.p.i. v.PAA reactivation titres are significantly lower than v.kLANA (* p-value<0.05, Mann-Whitney test). No other significant differences were observed between groups (p-value>0.05, Mann-Whitney test).

In addition to the infectious centre assay, a limiting dilution assay was performed to evaluate the presence of viral DNA in splenocytes and the frequency of infected cells. This assay is based on the serial dilution of known numbers of spleenocytes from infected mice and the detection of viral DNA by qPCR with primers and a probe specific for the MHV-68 M9 gene (Figure 3.5, Table 3.3). This assay provides an independent measure of latency since the results are not dependent on the ability of the virus to reactivate *ex vivo* but only on the presence of viral DNA.

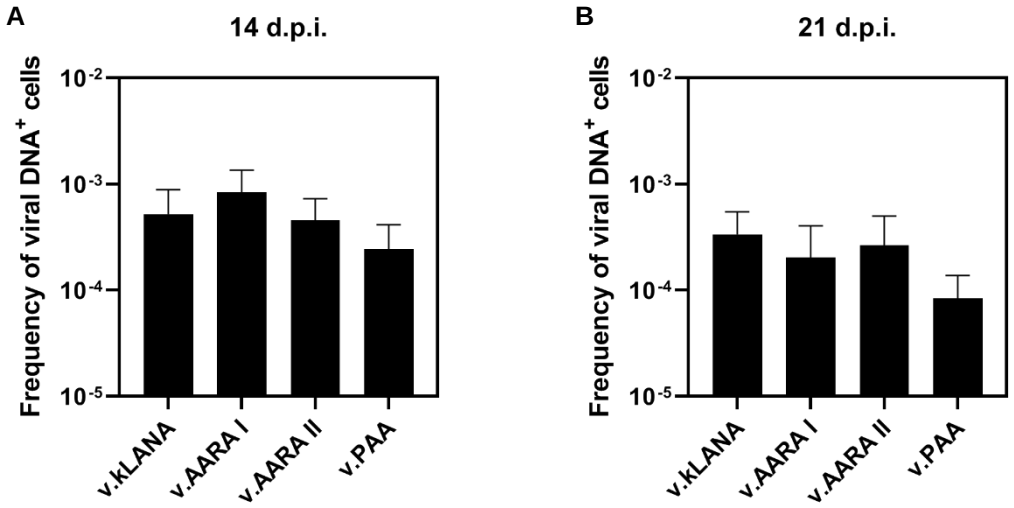

Figure 3.5 – Quantification of viral DNA-positive cells in total splenocytes. Balb/c mice were inoculated intranasally with 10^4 PFUs in 20 µL of PBS of v.kLANA, v.AARA I, v.AARA II and v.PAA. Mice were sacrificed at (A) 14 and (B) 21 d.p.i. and spleens were harvested. Spleens were processed and frequencies determined by the limiting dilution assay coupled with qPCR. Data are from pools of four mice. Bars represent the frequency of viral DNA-positive cells. Error bars indicate 95% confidence intervals.

Table 3.3 – Reciprocal frequency of viral DNA positive cells in total splenocytes[a].

Cell population	D.p.i.	Virus	Reciprocal frequency[b] of viral DNA positive cells (95% confidence interval)
Total spleenocytes	14	v.kLANA	1927 (1131-6516)
		v.AARA I	1194 (738-3114)
		v.AARA II	2200 (1377-5467)
		v.PAA	4112 (2412-13916)
	21	v.kLANA	2981 (1819-8260)
		v.AARA I	4908 (2476-27801)
		v.AARA II	3753 (1996-31468)
		v.PAA	11924 (7275-33039)

[a] Data was obtained from pools of four mice per group.

[b] Frequencies were determined by the limiting dilution assay coupled with qPCR, with 95% confidence intervals.

The results from this assay corroborate the results from the reactivation assay, showing that v.kLANA was able to establish latent infection and v.AARA I and v.AARA II behave similarly to one another and to v.kLANA, at 14 and 21 d.p.i.. Furthermore, v.PAA has a slightly lower frequency of viral DNA positive

cells than v.kLANA at 14 d.p.i., a difference that continues to show and is more marked at 21 d.p.i, as observed above (Figure 3.5, Table 3.3). These results indicate this mutation leads to reduced lifelong infection.

CHAPTER FOUR:

DISCUSSION AND FUTURE PERSPECTIVES

Viruses and their related diseases, as we observed this past year with SARS-CoV-2, can have a huge impact on our society, making research into these organisms incredibly necessary. Viral diseases come in several different forms, from respiratory pathologies, to hepatitis, to cancer. As of this moment, seven viruses have revealed oncogenic properties in humans and studying them has provided important insights into cancer causes, both infectious and non-infectious, giving rise to diagnostic, prevention and treatment targets that have helped in decreasing cancer development[65].

KSHV is a human herpesvirus that has been associated with several cancerous pathologies and for which there is no effective treatment currently, considering this virus is found mostly in a latent phase and most anti-viral therapies are targeted towards the lytic phase[66]. In order to effectively find therapy targets in the latent phase, it is necessary to understand the mechanisms behind the establishment and maintenance of latency which, for KSHV, relies heavily on kLANA[17]. Among its many functions, kLANA is able to affect chromatin modification through the interaction with histone methyltransferases (HMT), including the MLL1 complex[35,36,38].

In this study, to research the relevance of this interaction in the establishment of latency *in vivo*, two recombinant viruses were studied using the chimera kLANA-MHV-68 model developed in the lab[53], v.AARA, designed to increase affinity between the MLL1 complex and kLANA, and v.PAA, designed to impair this interaction. *In vitro* results, protein expression and growth kinetics, showed recombinant viruses were successfully reconstituted, were expressing the kLANA protein and had normal growth kinetics as expected, since LANA is not essential for virus lytic phase[52].

In vivo results show recombinant viruses can successfully establish lytic infection in the lungs similar to v.kLANA, confirming *in vitro* results. However, latent infection results showed that impairing the interaction between kLANA and WDR5 (v.PAA) reduced viral ability to establish latency, most especially long term. These results were somewhat expected, considering the recent studies detailing the interaction *in vitro* between kLANA and WDR5 from the MLL1 complex, TR histone tri-methylation by MLL1, and the resulting viral DNA degradation observed in the absence of MLL1 activity (unpublished results).

On the one hand, impairing kLANA-WDR5 interaction (v.PAA) led to a reduced latency phenotype, most markedly at 21 d.p.i.. These results corroborate the mechanism proposed for the consequences of kLANA-WDR5 interaction, where this interaction disrupts MLL1 activity in a dose-dependent manner, ensuring there is little to no tri-methylation of TR histones. In turn, this leads to no DNAse activity, thus, no viral DNA degradation through this pathway, allowing the virus to establish the latency program. This mechanism occurs in the first h.p.i. in cells, after which other viral protective mechanisms are activated,

stopping further DNA degradation. In suppressing kLANA-WDR5 interaction, reduced latency was observed, which was expected according to the mechanism described. Since kLANA could not interact with WDR5, this protein was able to support the establishment of the MLL1 complex, which tri-methylated the viral DNA. This chromatin modification led to viral DNA degradation which in turn resulted in lowered latency levels. Latency was not completely disrupted due to yet unknown viral DNA protective mechanisms that are activated later in infection.

On the other hand, increasing kLANA's affinity to WDR5 (v.AARA) didn't result in an observable phenotype. This was not necessarily expected since by increasing the affinity between kLANA and WDR5, MLL1 activity, and thus, TR tri-methylation should have decreased leading to less episome degradation and heightened latency levels. One possible explanation is that a threshold level of episome copy number in cells has been reached with non-mutant kLANA and that the increase in affinity between kLANA and WDR5, while decreasing MLL1 activity and viral DNA degradation, did not lead to an increase in episome copy numbers. Another possibility relates to whether mutated kLANA truly had an increased affinity towards WDR5. Although the kLANA WIN-like motif is now more similar to MLL1 WIN, the conformation of kLANA N-terminal might not allow for an increase in affinity towards WDR5.

In order to further clarify and confirm these results further experiments should be performed. As a starting point, independently derived mutants for v.PAA should be tested *in vivo*. Following this, chimeric recombinant viruses with a YFP background could be constructed and also tested *in vivo*. This background doesn't have an effect on *in vivo* infection, further confirming the results obtained. Furthermore, the YFP background allows for the tracking of infection through flow cytometry analysis and latently infected GC B cells can be quantified as well as the quantification of the number of episome copies per infected splenocyte. The latter would provide further insights on the mechanisms behind these results and the effects of the mutations in a single cell. Additionally, viral genome methylation could be evaluated in sorted cells.

Moreover, since the mechanism affected by these mutations involves chromatin modification following these modifications in the presence of mutated kLANA could provide further insights into this pathway, it could also be interesting to investigate whether these mutations lead to altered latency kinetics, where the peak of infection in the spleen was either before or after 14 d.p.i. and whether after more time than 21 d.p.i. it was still possible to detect viral DNA in infected spleens.

In conclusion, this work has corroborated the defence mechanism proposed for the relevance of MLL1 activity, tri-methylation and viral DNA degradation in infection by KSHV. Further work is needed to unveil this mechanism and its importance *in* vivo in order to develop novel therapies for latent KSHV infection.

REFERENCES

1. Lussignol, M. & Esclatine, A. Herpesvirus and autophagy: “All right, everybody be cool, this is a robbery!” *Viruses* **9**, (2017).
2. Cohrs, R. J. & Gilden, D. H. Human Herpesvirus Latency. *Brain Pathol.* **11**, 465–474 (2001).
3. Bharucha, T., Houlihan, C. F. & Breuer, J. Herpesvirus Infections of the Central Nervous System. *Semin. Neurol.* **39**, 369–382 (2019).
4. Mettenleiter, T. C., Klupp, B. G. & Granzow, H. Herpesvirus assembly: An update. *Virus Res.* **143**, 222–234 (2009).
5. Pellett, P. E. & Roizman, B. Herpesviridae. in *Fields Virology* (eds. Knipe, D. M. & Howley, P. M.) 1802–1822 (Lippincott Williams & Wilkins, 2013).
6. Davison, A. J. *et al.* The order Herpesvirales. *Arch. Virol.* **154**, 171–177 (2009).
7. Chandran, B. Early Events in Kaposi’s Sarcoma-Associated Herpesvirus Infection of Target Cells. *J. Virol.* **84**, 2188–2199 (2010).
8. Chang, Y. *et al.* Identification of herpesvirus-like DNA sequences in AIDS-associated Kaposi’s sarcoma. *Science (80-.).* **266**, 1865–1869 (1994).
9. Ueda, K. KSHV genome replication and maintenance in latency. in *Advances in Experimental Medicine and Biology* vol. 1045 299–320 (Springer New York LLC, 2018).
10. Cesarman, E. Gammaherpesviruses and Lymphoproliferative Disorders. *Annu. Rev. Pathol. Mech. Dis.* **9**, 349–372 (2014).
11. Yan, L., Majerciak, V., Zheng, Z. M. & Lan, K. Towards Better Understanding of KSHV Life Cycle: from Transcription and Posttranscriptional Regulations to Pathogenesis. *Virol. Sin.* **34**, 135–161 (2019).
12. Cai, Q., Verma, S. C., Lu, J. & Robertson, E. S. Molecular Biology of Kaposi’s Sarcoma-associated Herpesvirus and Related Oncogenesis. in *Advances in Virus Research* vol. 78 87–142 (Elsevier Inc., 2010).
13. Minhas, V. & Wood, C. Epidemiology and transmission of kaposi’s sarcoma-associated herpesvirus. *Viruses* **6**, 4178–4194 (2014).
14. Cesarman, E., Chang, Y., Moore, P. S., Said, J. W. & Knowles, D. M. Kaposi’s Sarcoma–Associated Herpesvirus-Like DNA Sequences in AIDS-Related Body-Cavity–Based Lymphomas. *N. Engl. J. Med.* **332**, 1186–1191 (1995).
15. Soulier, J. *et al.* Kaposi’s sarcoma-associated herpesvirus-like DNA sequences in multicentric Castleman’s disease. *Blood* **86**, 1276–1280 (1995).
16. Uldrick, T. S. *et al.* An interleukin-6-related systemic inflammatory syndrome in patients co-infected with kaposi sarcoma-associated herpesvirus and HIV but without multicentric

castleman disease. *Clin. Infect. Dis.* **51**, 350–358 (2010).

17. Juillard, F., Tan, M., Li, S. & Kaye, K. M. Kaposi's sarcoma herpesvirus genome persistence. *Front. Microbiol.* **7**, 1149 (2016).

18. Veettil, M. V., Bandyopadhyay, C., Dutta, D. & Chandran, B. Interaction of KSHV with host cell surface receptors and cell entry. *Viruses* **6**, 4024–4046 (2014).

19. Campbell, M., Yang, W. S., Yeh, W. W., Kao, C. H. & Chang, P. C. Epigenetic Regulation of Kaposi's Sarcoma-Associated Herpesvirus Latency. *Front. Microbiol.* **11**, 1–11 (2020).

20. Mesri, E. A., Cesarman, E. & Boshoff, C. Kaposi's sarcoma and its associated herpesvirus. *Nat. Rev. Cancer* **10**, 707–719 (2010).

21. Uppal, T., Banerjee, S., Sun, Z., Verma, S. C. & Robertson, E. S. KSHV LANA—The Master Regulator of KSHV Latency. *Viruses* **6**, 4691–4998 (2014).

22. De Leo, A. *et al.* LANA oligomeric architecture is essential for KSHV nuclear body formation and viral genome maintenance during latency. *PLOS Pathog.* **15**, e1007489 (2019).

23. Wei, F., Zhu, Q., Ding, L., Liang, Q. & Cai, Q. Manipulation of the host cell membrane by human γ-herpesviruses EBV and KSHV for pathogenesis. *Virol. Sin.* **31**, 395–405 (2016).

24. Lieberman, P. M. Keeping it quiet: Chromatin control of gammaherpesvirus latency. *Nat. Rev. Microbiol.* **11**, 863–875 (2013).

25. Uppal, T., Jha, H. C., Verma, S. C. & Robertson, E. S. Chromatinization of the KSHV genome during the KSHV life cycle. *Cancers (Basel).* **7**, 112–142 (2015).

26. Toth, Z. *et al.* Biphasic Euchromatin-to-Heterochromatin Transition on the KSHV Genome Following De Novo Infection. *PLoS Pathog.* **9**, e1003813 (2013).

27. Günther, T. & Grundhoff, A. The Epigenetic Landscape of Latent Kaposi Sarcoma-Associated Herpesvirus Genomes. *PLoS Pathog.* **6**, e1000935 (2010).

28. Krishnan, H. H. *et al.* Concurrent Expression of Latent and a Limited Number of Lytic Genes with Immune Modulation and Antiapoptotic Function by Kaposi's Sarcoma-Associated Herpesvirus Early during Infection of Primary Endothelial and Fibroblast Cells and Subsequent Decline of L. *J. Virol.* **78**, 3601–3620 (2004).

29. Ponnusamy, R. *et al.* KSHV but not MHV-68 LANA induces a strong bend upon binding to terminal repeat viral DNA. *Nucleic Acids Res.* **43**, 10039–10054 (2015).

30. Verma, S. C., Lan, K. & Robertson, E. Structure and function of latency-associated nuclear antigen. *Curr. Top. Microbiol. Immunol.* **312**, 101–136 (2007).

31. Barbera, A. J. *et al.* The nucleosomal surface as a docking station for Kaposi's sarcoma herpesvirus LANA. *Science (80-.).* **311**, 856–861 (2006).

32. Chiu, Y. F., Sugden, A. U., Fox, K., Hayes, M. & Sugden, B. Kaposi's sarcoma-associated herpesvirus stably clusters its genomes across generations to maintain itself

extrachromosomally. *J. Cell Biol.* **216**, 2745–2758 (2017).

33. Ohsaki, E. & Ueda, K. Kaposi's sarcoma-associated herpesvirus genome replication, partitioning, and maintenance in latency. *Front. Microbiol.* **3**, (2012).

34. Juillard, F., De León Vázquez, E., Tan, M., Li, S. & Kaye, K. M. Kaposi's Sarcoma-Associated Herpesvirus LANA-Adjacent Regions with Distinct Functions in Episome Segregation or Maintenance. *J. Virol.* **93**, 2158–2176 (2019).

35. Sakakibara, S. *et al.* Accumulation of Heterochromatin Components on the Terminal Repeat Sequence of Kaposi's Sarcoma-Associated Herpesvirus Mediated by the Latency-Associated Nuclear Antigen. *J. Virol.* **78**, 7299–7310 (2004).

36. Kim, K. Y. *et al.* Kaposi's Sarcoma-Associated Herpesvirus (KSHV) Latency-Associated Nuclear Antigen Regulates the KSHV Epigenome by Association with the Histone Demethylase KDM3A. *J. Virol.* **87**, 6782–6793 (2013).

37. Hu, J. *et al.* LANA Binds to Multiple Active Viral and Cellular Promoters and Associates with the H3K4Methyltransferase hSET1 Complex. *PLoS Pathog.* **10**, e1004240 (2014).

38. Toth, Z. *et al.* LANA-Mediated Recruitment of Host Polycomb Repressive Complexes onto the KSHV Genome during De Novo Infection. *PLOS Pathog.* **12**, e1005878 (2016).

39. Park, S. H. *et al.* Cryo-EM structure of the human MLL1 core complex bound to the nucleosome. *Nat. Commun.* **10**, 1–13 (2019).

40. Li, Y. *et al.* Structural basis for activity regulation of MLL family methyltransferases. *Nature* **530**, 447–452 (2016).

41. Patel, A., Vought, V. E., Dharmarajan, V. & Cosgrove, M. S. A conserved arginine-containing motif crucial for the assembly and enzymatic activity of the mixed lineage leukemia protein-1 core complex. *J. Biol. Chem.* **283**, 32162–32175 (2008).

42. Zhang, P., Lee, H., Brunzelle, J. S. & Couture, J. F. The plasticity of WDR5 peptide-binding cleft enables the binding of the SET1 family of histone methyltransferases. *Nucleic Acids Res.* **40**, 4237–4246 (2012).

43. Pedro Simas, J. & Efstathiou, S. Murine gammaherpesvirus 68: A model for the study of gammaherpesvirus pathogenesis. *Trends Microbiol.* **6**, 276–282 (1998).

44. Stevenson, P. G. & Efstathiou, S. Immune mechanisms in murine gammaherpesvirus-68 infection. *Viral Immunol.* **18**, 445–456 (2005).

45. Blaskovic, D., Stanceková, M., Svobodová, J. & Mistríková, J. Isolation of five strains of herpesviruses from two species of free living small rodents. *Acta Virologica* vol. 24 468 (1980).

46. Milho, R. *et al.* In vivo imaging of murid herpesvirus-4 infection. *J. Gen. Virol.* **90**, 21–32 (2009).

47. Mistríková, J. & Briestenská, K. Murid herpesvirus 4 (MuHV-4, prototype strain MHV-68) as an important model in global research of human oncogenic gammaherpesviruses. *Acta Virol.* **64**,

167–176 (2020).

48. Pires de Miranda, M., Quendera, A. P., McVey, C. E., Kaye, K. M. & Simas, J. P. In Vivo Persistence of Chimeric Virus after Substitution of the Kaposi's Sarcoma-Associated Herpesvirus LANA DNA Binding Domain with That of Murid Herpesvirus 4 . *J. Virol.* **92**, 1251–1269 (2018).

49. Habison, A. C., Beauchemin, C., Simas, J. P., Usherwood, E. J. & Kaye, K. M. Murine Gammaherpesvirus 68 LANA Acts on Terminal Repeat DNA To Mediate Episome Persistence. *J. Virol.* **86**, 11863–11876 (2012).

50. Virgin, H. W. *et al.* Complete sequence and genomic analysis of murine gammaherpesvirus 68. *J. Virol.* **71**, 5894–5904 (1997).

51. Gupta, A., Oldenburg, D. G., Salinas, E., White, D. W. & Forrest, J. C. Murine Gammaherpesvirus 68 Expressing Kaposi Sarcoma-Associated Herpesvirus Latency-Associated Nuclear Antigen (LANA) Reveals both Functional Conservation and Divergence in LANA Homologs. *J. Virol.* **91**, 992–1009 (2017).

52. Fowler, P., Marques, S., Simas, J. P. & Efstathiou, S. ORF73 of murine herpesvirus-68 is critical for the establishment and maintenance of latency. *J. Gen. Virol.* **84**, 3405–3416 (2003).

53. Habison, A. C. *et al.* Cross-species conservation of episome maintenance provides a basis for in vivo investigation of Kaposi's sarcoma herpesvirus LANA. *PLOS Pathog.* **13**, e1006555 (2017).

54. Warden, C., Tang, Q. & Zhu, H. Herpesvirus BACs: Past, present, and future. *J. Biomed. Biotechnol.* **2011**, 16 (2011).

55. Adler, H., Messerle, M., Wagner, M. & Koszinowski, U. H. Cloning and Mutagenesis of the Murine Gammaherpesvirus 68 Genome as an Infectious Bacterial Artificial Chromosome. *J. Virol.* **74**, 6964–6974 (2000).

56. Stevenson, P. G. *et al.* K3-mediated evasion of CD8+ T cells aids amplification of a latent γ-herpesvirus. *Nat. Immunol.* **3**, 733–740 (2002).

57. Efstathiou, S., Ho, Y. M. & Minson, A. C. Cloning and molecular characterization of the murine herpesvirus 68 genome. *J. Gen. Virol.* **71**, 1355–1364 (1990).

58. Adler, H., Messerle, M. & Koszinowski, U. H. Virus Reconstituted from Infectious Bacterial Artificial Chromosome (BAC)-Cloned Murine Gammaherpesvirus 68 Acquires Wild-Type Properties In Vivo Only after Excision of BAC Vector Sequences. *J. Virol.* **75**, 5692–5696 (2001).

59. Pires De Miranda, M., Lopes, F. B., McVey, C. E., Bustelo, X. R. & Simas, J. P. Role of Src homology domain binding in signaling complexes assembled by the murid γ-herpesvirus M2 protein. *J. Biol. Chem.* **288**, 3858–3870 (2013).

60. Ryu, W.-S. Diagnosis and Methods. in *Molecular Virology of Human Pathogenic Viruses* 47–62

(2017). doi:10.1016/b978-0-12-800838-6.00004-7.

61. Bonnefoix, T., Bonnefoix, P., Callanan, M., Verdiel, P. & Sotto, J.-J. Graphical Representation of a Generalized Linear Model-Based Statistical Test Estimating the Fit of the Single-Hit Poisson Model to Limiting Dilution Assays. *J. Immunol.* **167**, 5725–5730 (2001).

62. Marques, S., Efstathiou, S., Smith, K. G., Haury, M. & Simas, J. P. Selective Gene Expression of Latent Murine Gammaherpesvirus 68 in B Lymphocytes. *J. Virol.* **77**, 7308–7318 (2003).

63. Toptan, T., Fonseca, L., Kwun, H. J., Chang, Y. & Moore, P. S. Complex Alternative Cytoplasmic Protein Isoforms of the Kaposi's Sarcoma-Associated Herpesvirus Latency-Associated Nuclear Antigen 1 Generated through Noncanonical Translation Initiation. *J. Virol.* **87**, 2744–2755 (2013).

64. Canham, M. & Talbot, S. J. A naturally occurring C-terminal truncated isoform of the latent nuclear antigen of Kaposi's sarcoma-associated herpesvirus does not associate with viral episomal DNA. *J. Gen. Virol.* **85**, 1363–1369 (2004).

65. Moore, P. S. & Chang, Y. Why do viruses cause cancer? Highlights of the first century of human tumour virology. *Nature Reviews Cancer* vol. 10 878–889 (2010).

66. Chen, J. *et al.* Identification of new antiviral agents against Kaposi's sarcoma-associated herpesvirus (KSHV) by high-throughput drug screening reveals the role of histamine-related signaling in promoting viral lytic reactivation. *PLOS Pathog.* **15**, e1008156 (2019).